Identification of non-nucleoside human ribonucleotide reductase modulators

Md. Faiz Ahmad[1]$, Sarah E Huff[2]$, John Pink[3], Intekhab Alam[1] Andrew Zhang[1], Kay Perry[4], Michael E. Harris[5], Tessianna Misko[1], Suheel K. Porwal[8], Nancy L. Oleinick[3,6], Masaru Miyagi[9], Rajesh Viswanathan[2], Chris Godfrey Dealwis*[1,7]

SUPPORTING INFORMATION

Table of Contents

1

EXPERIMENTAL SECTION

Virtual screening of the Cincinnati library against hRRM1

In order to conduct virtual screening against hRRM1 we used a homology model of the dATP-induced hexamer, that was based on the *S.cerevisiae* hexamer structure (Fig 2A main text, [1]). The model was made by substituting the hRRM1 sequence onto the *S.cerevisiae* structure followed by energy minimization in Prime using OPLS force field.

Docking with Schrödinger

In silico docking of the University of Cincinnati drug library was performed using the Glide docking module of the Schrodinger 9.3 modeling software suite [2]. The hRRM1 hexamer structure was first refined using Prime. Common problems associated with modeling crystal structures, such as missing hydrogen atoms, incomplete side chains and loops, ambiguous protonation states, and flipped residues, are resolved before docking. Prime uses the Optimized Potentials for Liquid Simulations All-Atom (OPLS) force field and the Surface generalized Born (SGB) continuum solution model for optimization and minimization. Likewise, the Ligprep program was used to generate 3D structures from the 2D drug library using OPLS 2001 force field. Once the drug library and the protein structure were prepared, docking was performed with Glide through the virtual screening workflow provided in Maestro, narrowing the hits to the top

10% through each step of the screening process. The final Glide XP results were kept and analyzed by docking score. The hits were scored using a docking function and a glide scoring function (glide score). The docking function is comprised of a linear combination of nonlinear functions of entropic, solvation, steric and polar effects [2]. The Schrödinger docking score is such that more negative values reflect stronger binding. Docking scores of -5 are generally considered moderate binders, while compounds with scores of -10 are considered very strong binders. Top hits were visually inspected for interactions with the binding pocket. When determining hits, we carefully examined the docking poses (Fig S4) where common interactions were a good indication of a consensus binding site. For example, residues Ile 44, Gln 45, Met 1, His 2, Val 51, and Val 43 interact with all ten compounds in Table 1, which is a good indication that they are binding at the same site.

Ribonucleotide reductase inhibition assays

The specific activity of hRR was determined using *in vitro* ^{14}C-ADP reduction assays as previously described [1, 3]. The iron was loaded into the small subunit of RR as follows. The buffer solution (50 mM HEPES at pH 7.6, 5% (v/v) glycerol, 0.1M KCl) and the hRRM2 protein in the buffer solution were prepared under deoxygenated conditions. Both solutions were taken into the glove box and $FeNH_4SO_4$ was dissolved in the buffer solution. 5 equivalents of Fe (II) per hRRM2 dimer from $FeNH_4SO_4$ (determined by Ferrozine assay) was added to the protein solution and incubated at 4ºC in the glove box. Upon removal of the protein from the glove box, freshly prepared O_2-saturated buffer solution (50 mM HEPES at pH 7.6, 5% (v/v) glycerol, 0.1M KCl) was added. Excess iron was removed by S200 10/300 size exclusion chromatography. To determine the specific activity of hRRM1 we used a reaction mixture containing 0.3 µM hRRM1

and 2.1 µM hRRM2 in an activity assay buffer of 50 mM HEPES pH 7.6, 15 mM $MgCl_2$, 1 mM EDTA, 100 mM KCl, 5 mM DTT, 3 mM ATP, 100 µM dGTP and 1 mM ^{14}C-ADP (~3000 cpm/nmol). The reaction mixture was pre-incubated for 3 min at 37˚C, and 30 µL aliquots were sampled at fixed time intervals after initiating the reaction. Reactions were quenched by immersion in a boiling water bath, cooling, and treatment with alkaline phosphatase. The product ^{14}C-dADP that formed during the reaction was separated from substrate ^{14}C-ADP using boronate affinity chromatography [3]. ^{14}C-dADP was quantified by liquid scintillation counting using a Beckman LS6500 liquid scintillation counter. Since most of our compounds were dissolved in 100% DMSO, the loss of activity due to 0.2% DMSO, which is the final concentration of DMSO in the activity assay, was determined to be less than 1%, suggesting that it is almost negligible. The IC_{50} was defined as the concentration of any compound that reduced the specific activity of hRRM1 to 50% of the control activity. Since we had a limited amount of compound from the Cinncinnati library available, we adopted a two-point method for IC_{50} determination using the procedure described in Krippendorff 2007 *et. al.*, [4]. Based on this method, we used 5 and 25 µM concentrations of the ligand for measuring the $IC_{50.}$ All ligands tested were obtained from the University of Cincinnati chemical library as a 30 mM solution in 100% DMSO. The GRI Numbers, molecular weight, and the original manufacturer's source are listed for the each compound in Table S2. All structures provided are rendered with their specific stereochemistry identified unless the stereochemistry is unknown. Mass spectrometry analysis was performed using a LTQ-Orbitrap Velos mass spectrometer equipped with an electrospray ion source (Thermo-Finnigan, Bremen, Germany). The samples in 0.1% formic acid and 50% acetonitrile were introduced into the ion source at a flow rate of 5 µL/min and the full MS spectra of the produced ions were acquired at a resolution of 60,000 in the positive ion mode.

Inhibition mechanism

RR inhibition assays were performed as previously described for wt hRRM1 at inhibitor concentrations of 0, 32, and 64 μM of **Compound 4**. For all three inhibitor concentrations, the specific activity was recorded for substrate concentrations of 5, 1, 0.5, 0.2, 0.1, and 0.05 mM of ^{14}C-ADP. Each data set was recorded in duplicates. The velocity of each reaction was plotted against concentration of substrate and analyzed by the mixed-model equation in GraphPad Prism 6. The parameters V_{max}, K_m, K_i and α were constrained to be shared for all inhibitor concentrations. The mechanism of inhibition was determined by the alpha value, where α = 1 denotes noncompetitive inhibition, α >> 1 denotes competitive inhibition, and α << 1 denotes uncompetitive inhibition. A double reciprocal plot was also generated for the data set in GraphPad.

Growth Inhibition screening assays for determining cellular toxicity

Cell were maintained in standard tissue culture media (RPMI1640, + 10% fetal bovine serum, plus antibiotic) and grown in a standard humidified 5% CO2 incubator at 37˚C. Cells were regularly tested using the MycoAlert detection kit (Lonza Biologics) and shown to be mycoplasma-free. Initial compound screening was performed using both MDA-MB-231 (a generous gift of Dr. V.C. Jordan) and HCT-116 (a generous gift of Dr. Sandy Markowitz) cell lines. For moderate throughput screening (up to 120 drugs per experiment), cells were seeded into 96 well plates and allowed to attach overnight. The following day media was removed and replaced with fresh compound containing media. Each compound was tested against both cell lines at 3 concentrations; 1uM, 10uM and 50uM, in duplicate. Cells were incubated with compound containing media for three days in a standard 5% CO_2 tissue culture incubator. Cell growth was assessed after 3 days using the DNA dye binding assay, as originally described by

LaBarca and Paigen [5]. Relative growth was independently calculated for each cell line, based on DNA content from corresponding cells grown in control media plus diluent (DMSO). Additional growth inhibition experiments utilized either the DNA binding assay or the Promega CellTiter 96® (MTT reduction) assay, with similar results. For detailed growth inhibition assays, cells (1500-2500 depending on the growth characteristics of the cell line) were seeded in standard 96 well tissue culture plates and allowed to attach overnight. The following day media was removed and replaced with drug containing media. Each dose group consisted of 5 replicate wells, and results are reported as Relative Growth, calculated as DNA or MTT reduction per well, divided by the signal from untreated cells, both harvested 3 days after drug administration.

For the combination experiments a constant dose of **Compound 1** was co-administered with a standard dose range of gemcitabine. The dose of **Compound 1** used was the highest dose tested in each cell line that showed minimal or no growth inhibition as a single agent. Median effect doses (Dm) were calculated using Calcusyn version 2.0.

Crystallization of hRRM1

hRRM1 was crystallized in the orthorhombic $P2_12_12_1$ space group by the hanging drop vapor diffusion method at room temperature. Briefly, the well solution for crystallizations contained 0.1 M TRIS pH 7.9, 0.2 M Li_2SO_4, and 19% PEG-3350. The hanging drops contained 1 μL of protein solution at 20 mg/ml in 50 mM TRIS pH 8.0, 5% glycerol, 5 mM $MgCl_2$, 10 mM DTT, 20 mM TTP and 1 μL of the well solution. Initial co-crystallization attempts with **Compound 4** (a phthalamide derivative) did not yield any co-crystals. Hence we resorted to the soaking method. We used 100-500 μM compound in our soaking experiment. Crystals were incubated for 1-2h in reservoir solution containing 19% polyethylene glycol 3350, 0.2 M Li_2SO_4 and 100 mM Tris pH 7.9 with 100 -500 μM **Compound 4**. Subsequently, crystals were transferred to cryo-

protectant buffer (well solution + 20% glycerol) and then flash frozen in liquid nitrogen for data collection.

Data collection and structure determination

The data were collected from a flash-cooled crystal at cryogenic temperatures at the NECAT 24IDE beam line at the Advanced Photon Source using an ADSC Quantum-315 CCD detector. All the crystals belong to the orthorhombic space group $P2_12_12_1$, with unit cell parameter given in Table S6. The data were integrated and scaled using HKL 2000 [6]. The complex crystals are all isomorphous to the native $P2_12_12_1$ form (Protein Data Bank codes: 3HNC) and the structure was directly determined by the difference Fourier technique. The graphic software Coot [7] was used for model building interspersed with refinement using REFMAC5/PHENIX [8]. The final models were evaluated with PROCHECK [9]. The electron density for ligands was confirmed by calculating omit maps using the program PHENIX [8b, 10]. Figures were prepared in PyMOL [11].

Gel filtration chromatography
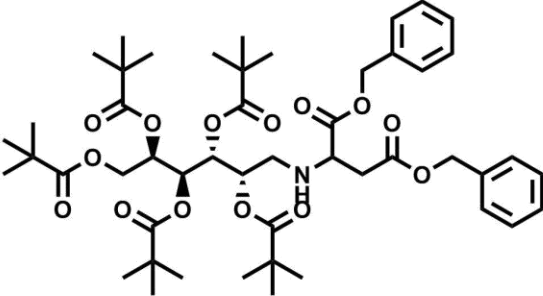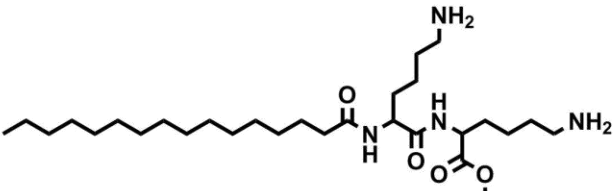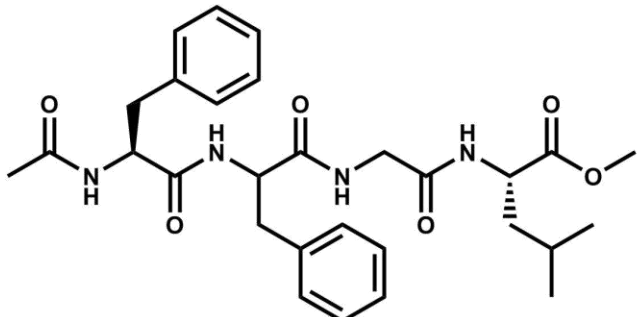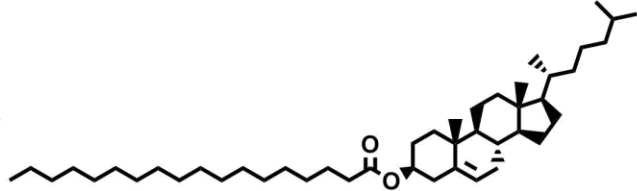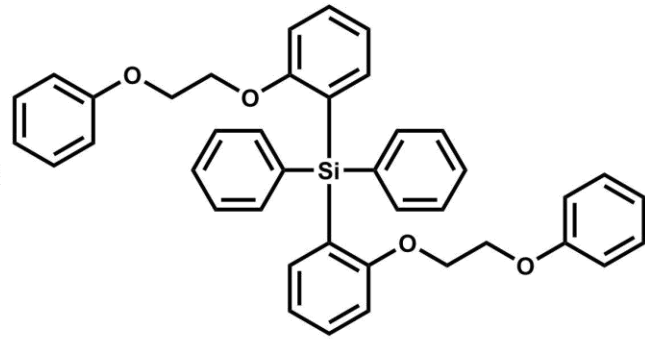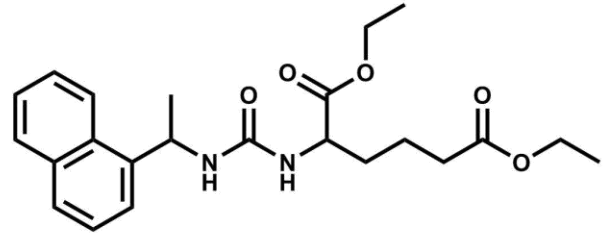
Gel filtration chromatography was conducted using a Superdex 10/300 GL column (GE Healthcare) containing a bed volume of 24 mLs. The column was equilibrated with two column volumes or more containing Buffer A (50mM Tris, pH 8.0, 5mM $MgCl_2$, 5% glycerol, 0.1 M KCl, 5mM DTT). Once a stable baseline was observed, hRRM1 samples at 10 µM were injected to obtain its chromatograph without nucleotide. To investigate the impact of the phthalimide compound (Table 1 main text, **Compound 4**) on oligomerization this inhibitor was incubated with hRMM1 at a concentration of 1mM prior to injection. The concentration of 1mM is approximately 30 times greater than its IC_{50} for hRRM1. It was felt that such a high concentration was needed to reduce the impact of the dilution, because the compound was not
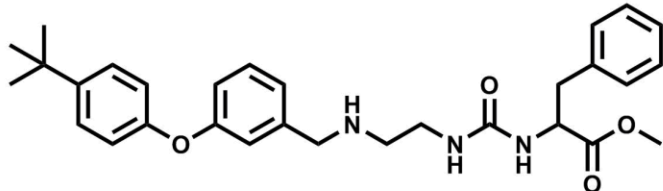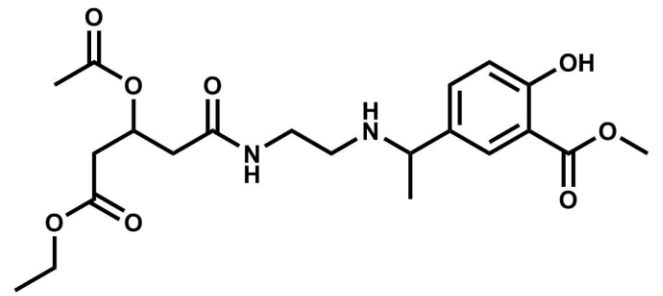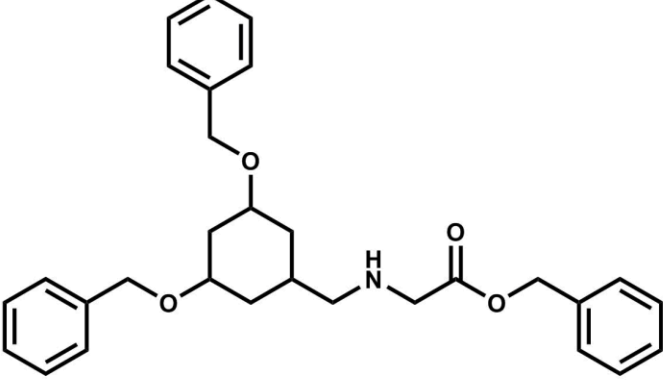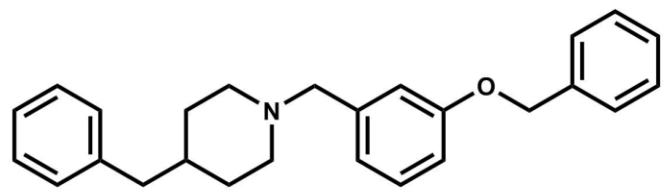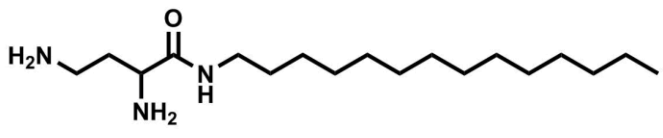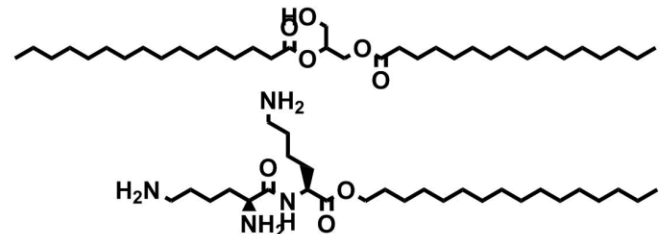
present in the equilibration buffer. The compound's impact on the dATP-induced oligomers was studied by incubating the compound with 50 µM dATP. For a control independent chromatographs were generated where only dATP was present at 50 µM concentrations. The column was calibrated using a low molecular weight standard as described [12]
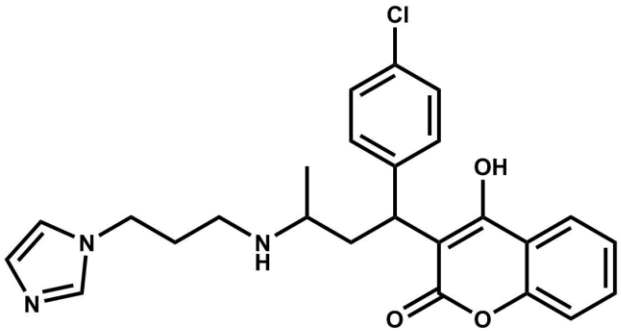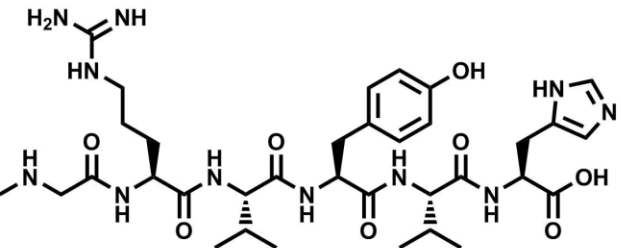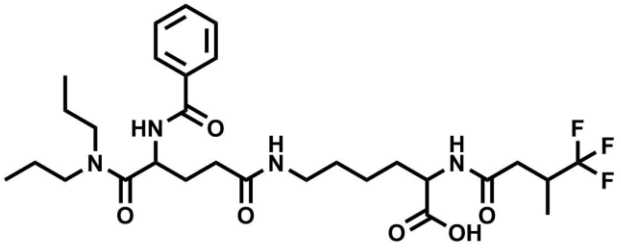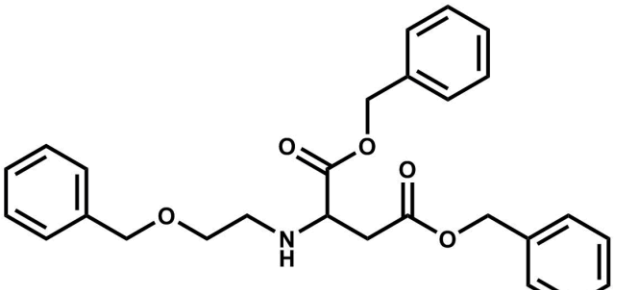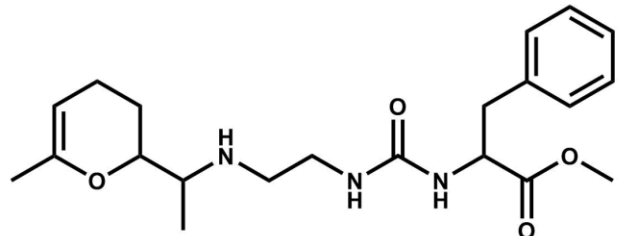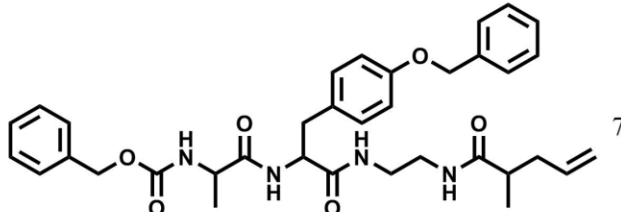
Tables and Figures
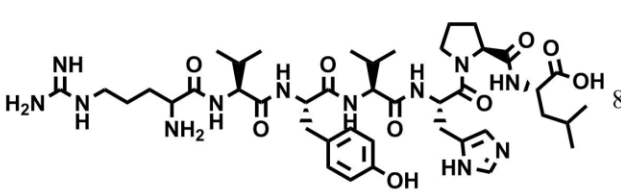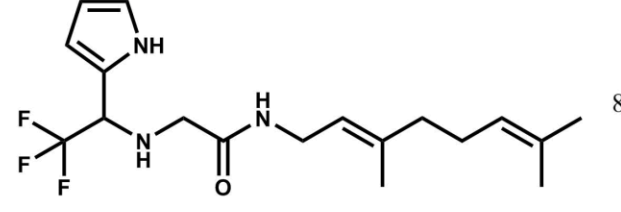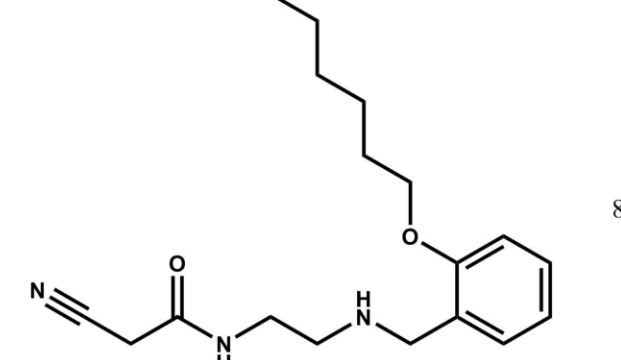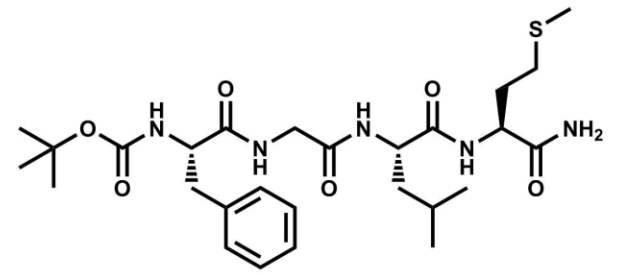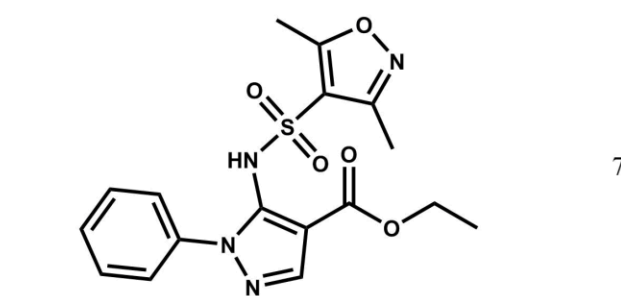
Table S1: Docking scores for the remaining 76 hits after 18 PAINS were eliminated from the top 94 hits. The SYBYL and Schrödingerdocking scores are reported as well as the percent quenching. Hits are ranked in descending order of SYBYL Surflex docking score. Quenching greater than 25% was used as the cutoff benchmark for establishing binding.
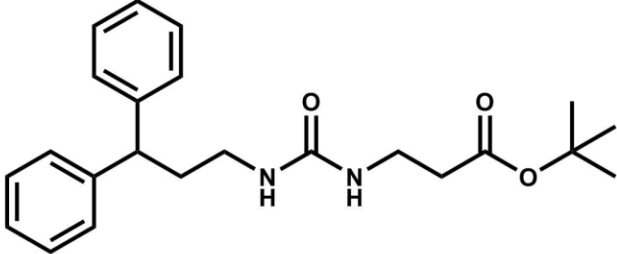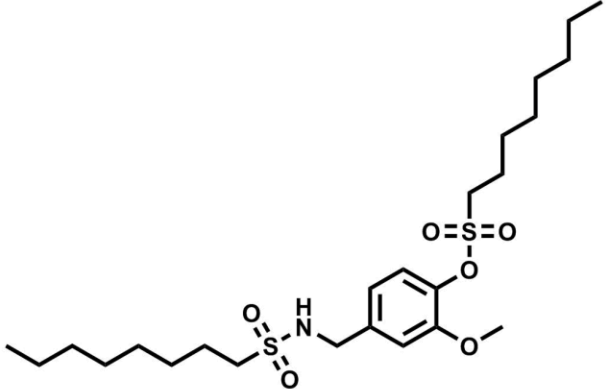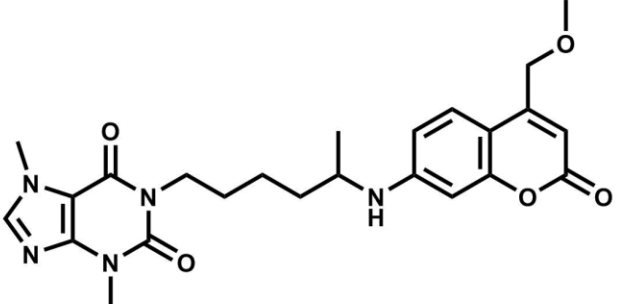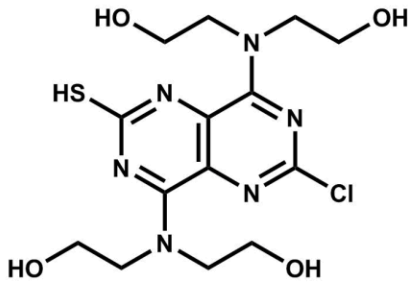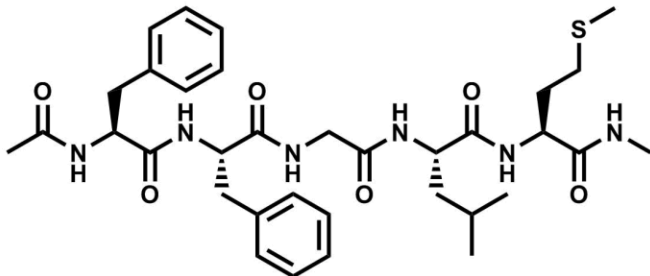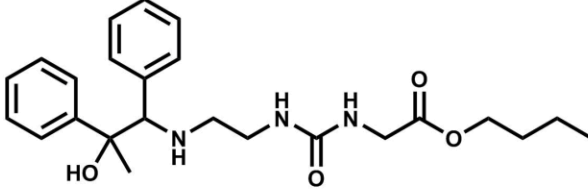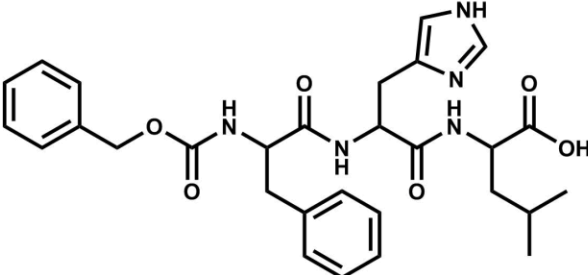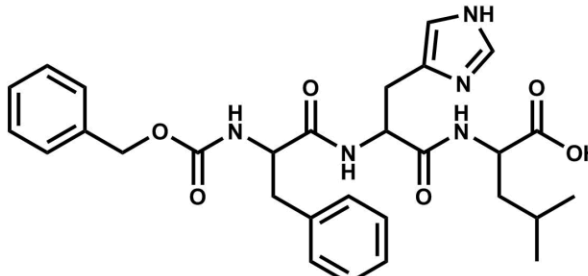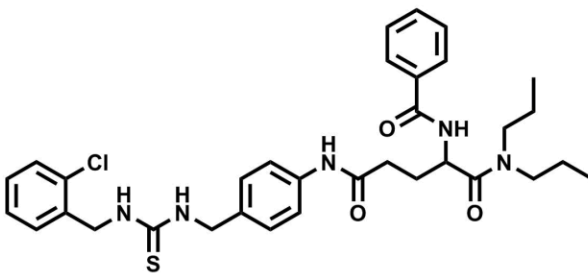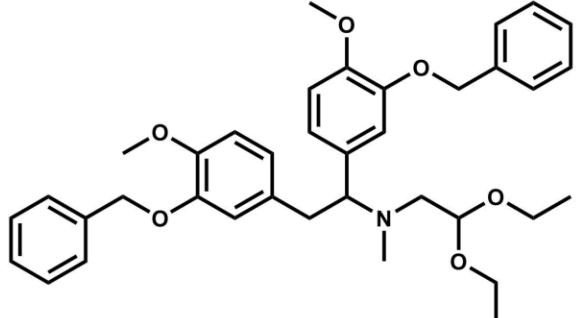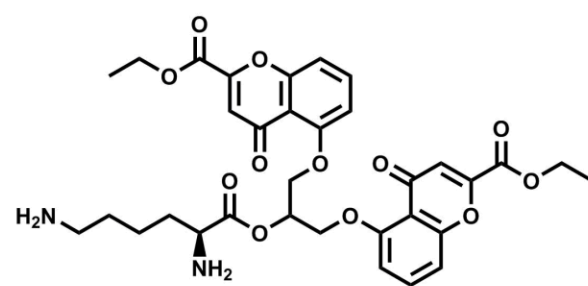
GRI Number	Structure	SYBYL Docking Score	Schrodinger Score	Percent Quenching
187884		9.57	-4.867	27
95889		9.18	-5.699	32
99069		9.14	-5.399	No quenching
299934		9.07	-4.155	11
257518		8.89	-4.082	10
156769		8.85	-4.717	20
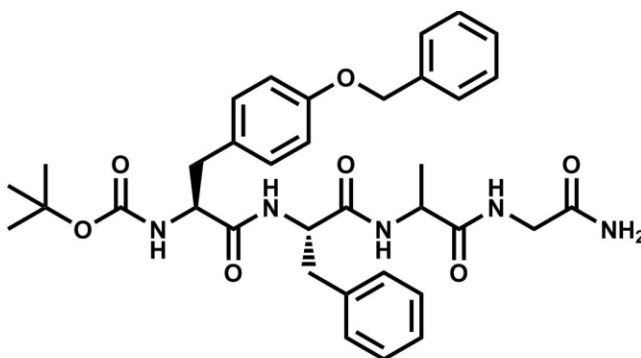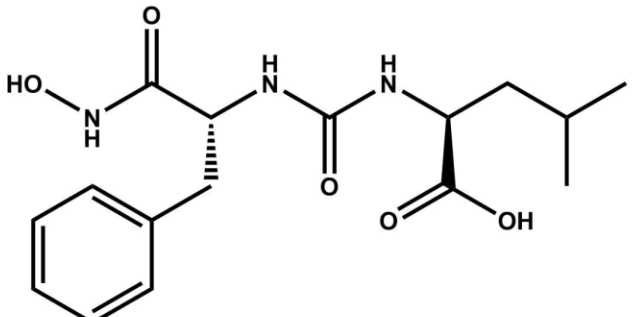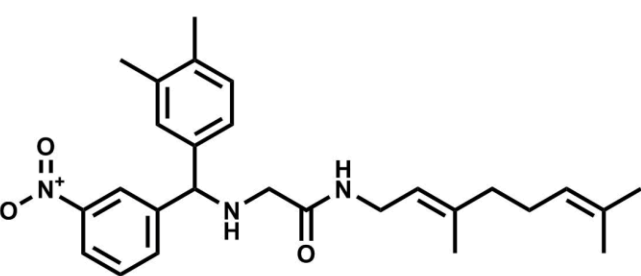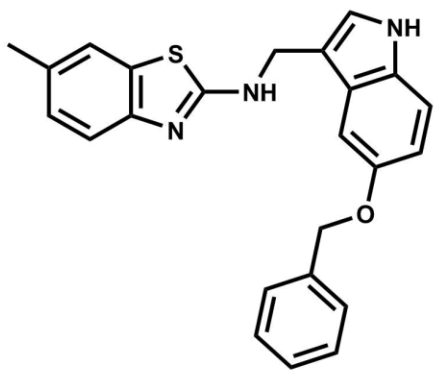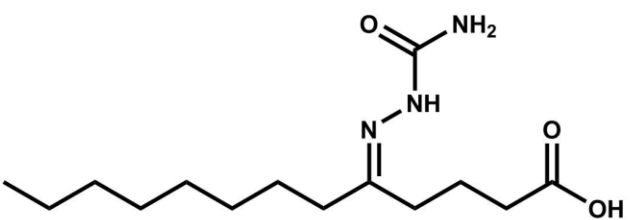
| 169994 | 8.69 | -4.942 | 15 |

| 169979 | 8.59 | -5.504 | 29 |

| 171956 | 8.45 | -4.871 | Not significant |

| 382907 | 7.01 | -5.08421 | 10 |

| 95946 | 8.39 | -4.59 | 33 |

| 95905 | 8.27 | -3.875 | 11 |
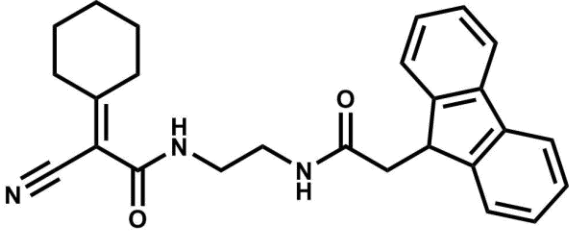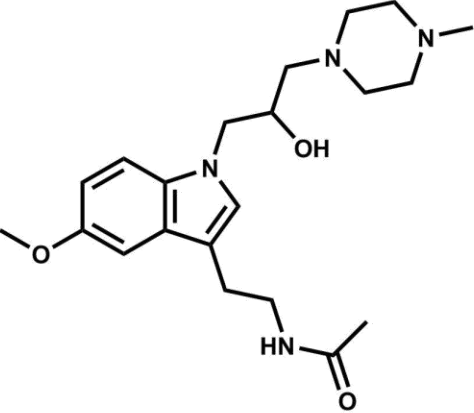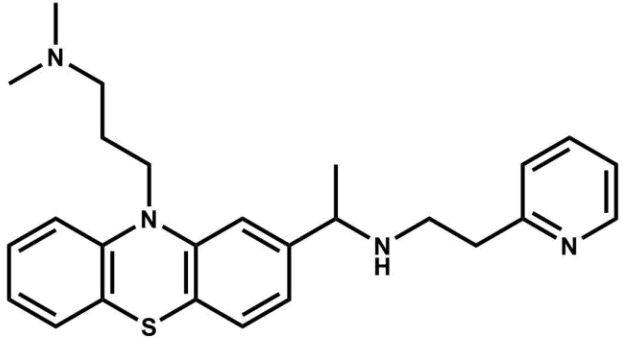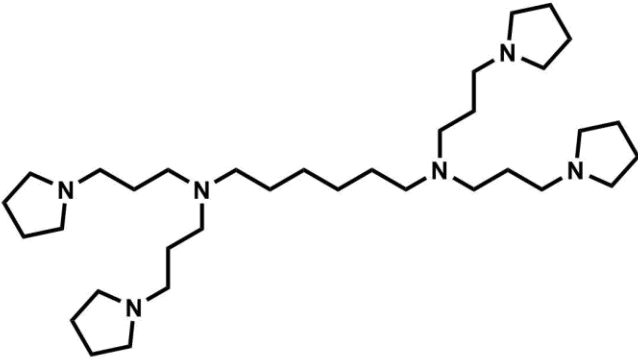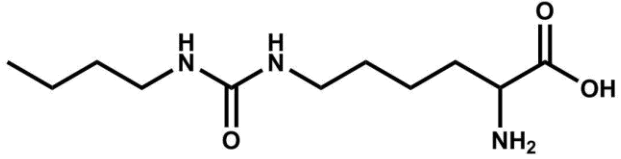
172757	8.24	-4.701	No quenching
97679	8.19	-5.042	43
184527	8.17	-4.951	10
187629	8.15	-5.035	15
170032	8.11	-5.334	22

100207		8.07	-5.365	No quenching
184612		8.07	-4.931	No quenching
170479		8.05	-3.537	10
99090		8	-4.632	Not significant
155516		7.06	-3.8609	38
170870		7.96	-4.40748	45
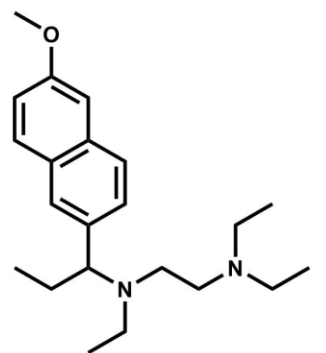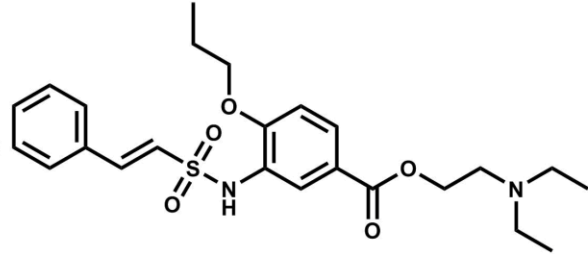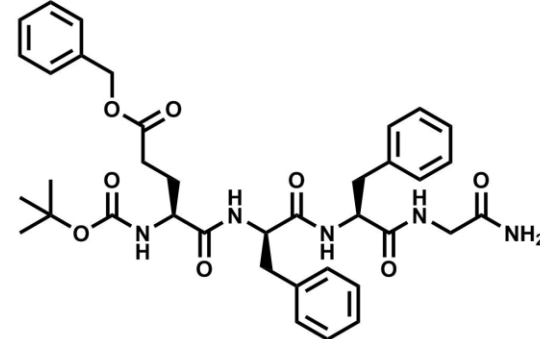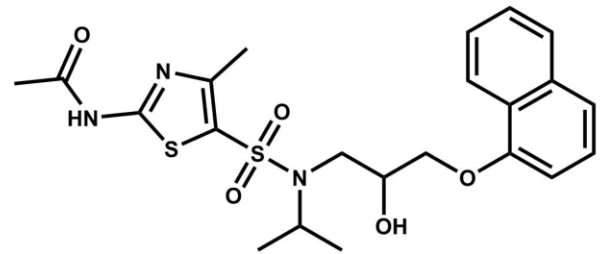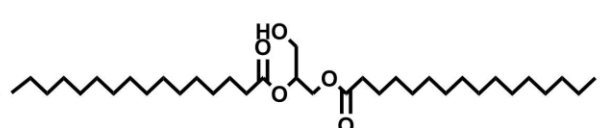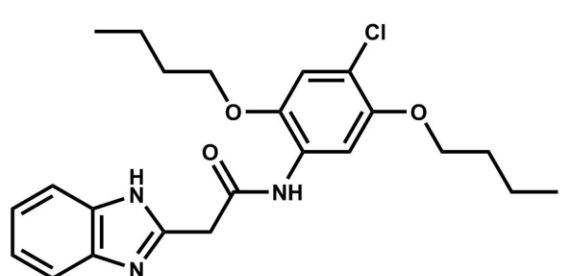
187931	7.96	-3.6226	Not significant
13425	7.92	-5.02586	20
186054	7.91	-5.36133	18
261191	7.91	-3.94716	10
99072	7.89	-6.88018	Not significant

13
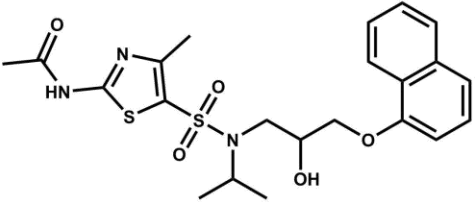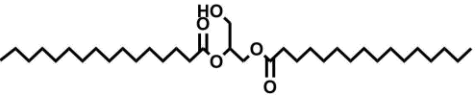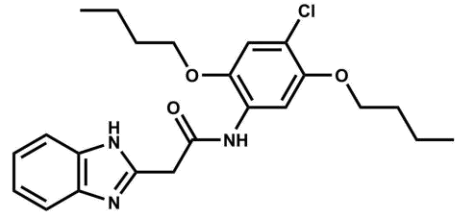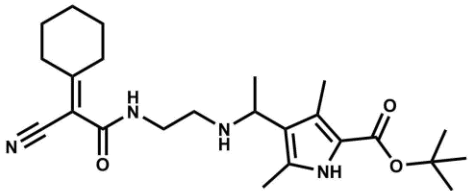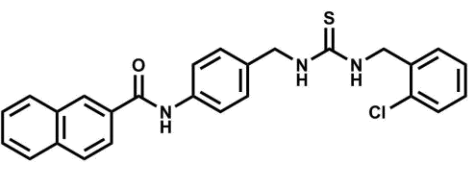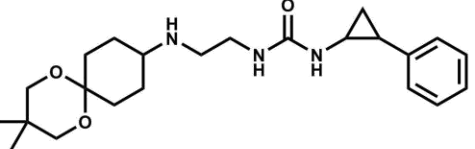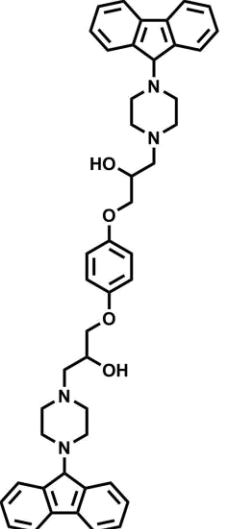
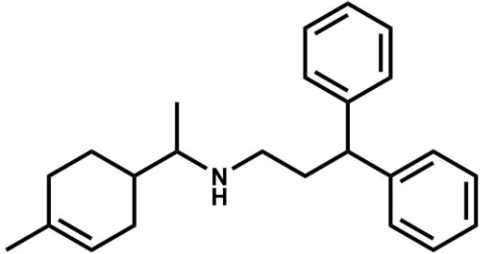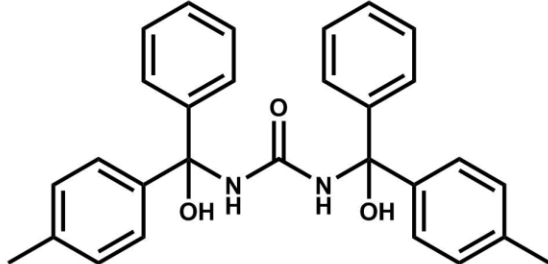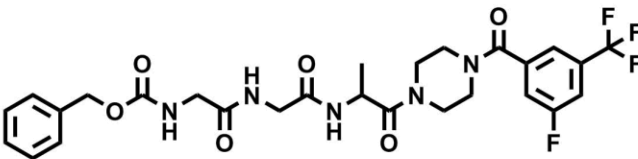|			
170096	7.89	-3.61111	No quenching
96005	7.88	-5.76766	Not significant
97567	7.88	-5.76766	No quenching
182759	7.88	-6.50553	15
251968	7.85	-4.50142	45
9370	7.13	-6.00874	25
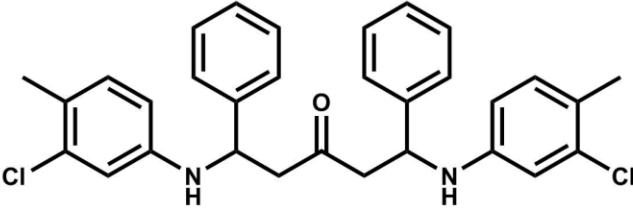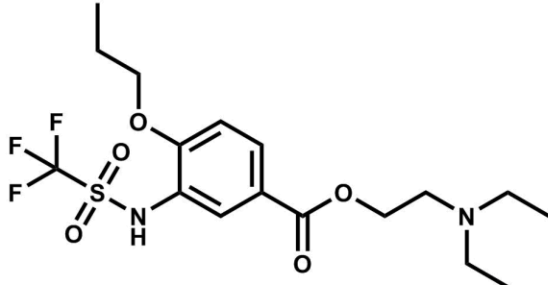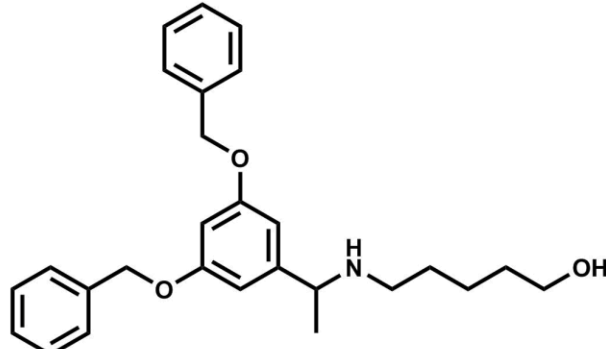
99364 7.84 -6.43763 5

100204 7.81 -4.03208 No quenching

185598 7.78 -3.67326 No quenching

190714 7.78 -4.6568

296755 7.78 -1.43685 23
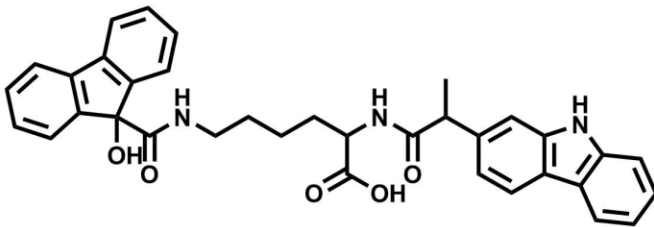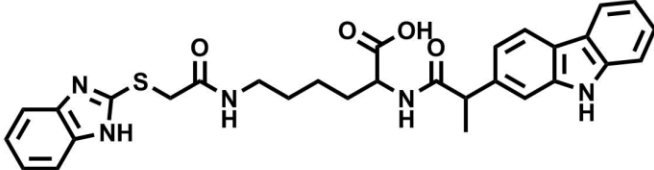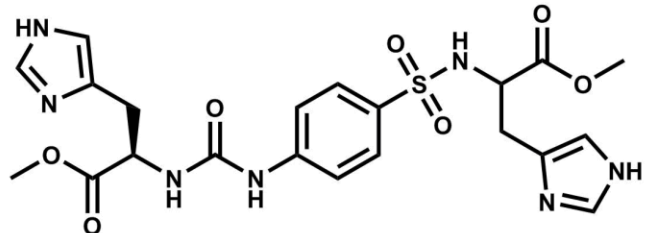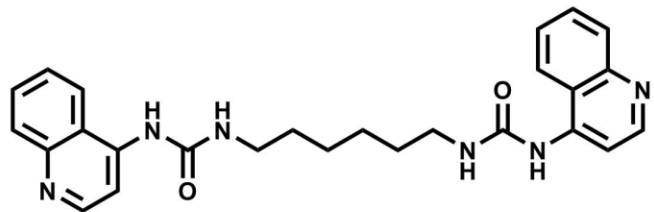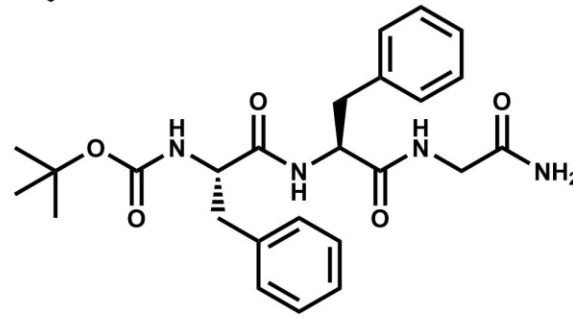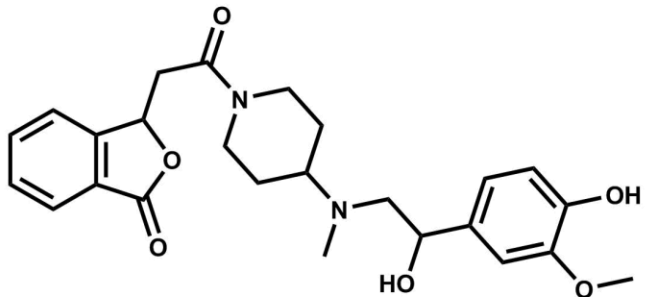
170802	7.77	-2.03396	50
128346	7.76	-6.86047	22
265472	7.73	-4.585	No quenching
279644	7.73	-5.79402	10
98467	7.72	-1.29271	Not significant

16
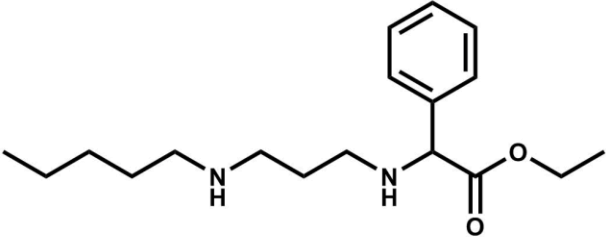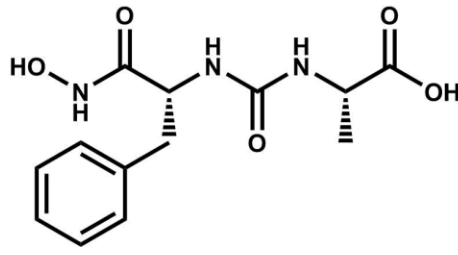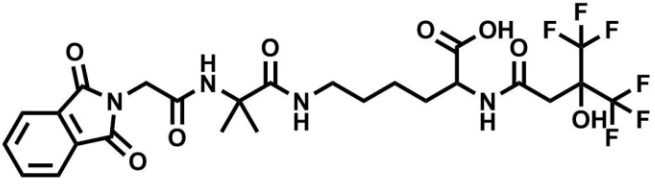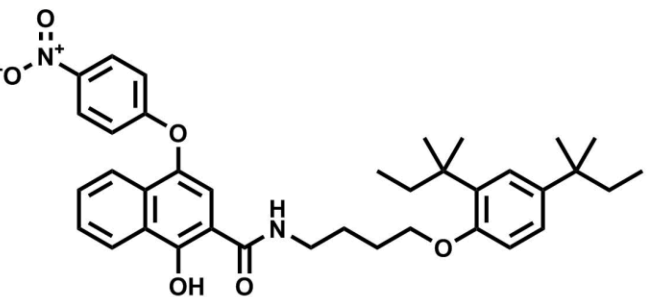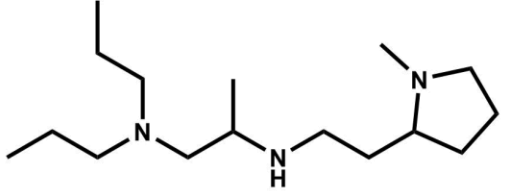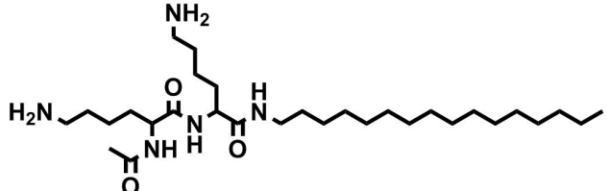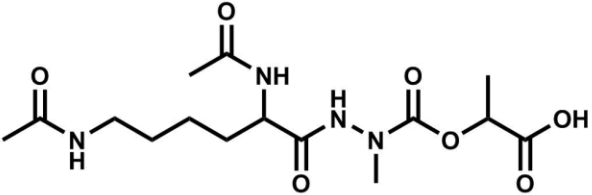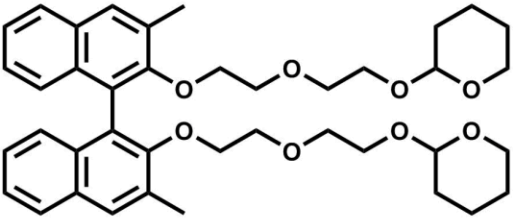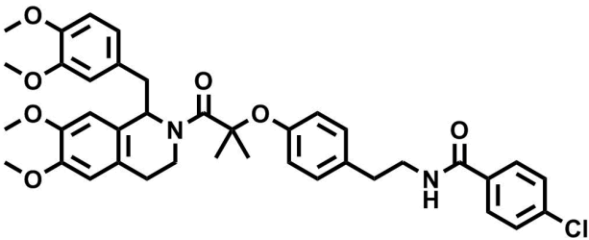
157875		7.7	-5.91556	No quenching
188275		7.67	-2.60787	50
99625		7.65	-6.31025	22
188109		7.18	-3.59204	Not significant
100604		7.22	-4.9972	20
96592		7.62	-3.40964	18

17

188109   7.18   -3.59204   Not significant

100604   7.22   -4.9972   20

96592   7.62   -3.40964   18

170674   7.54   -3.10278   15

182733   7.53   -5.04449   25

170317   7.52   -4.94688   20

193840   7.52   -6.8291   15
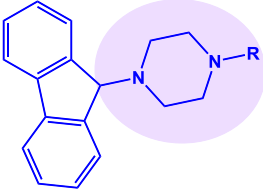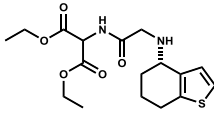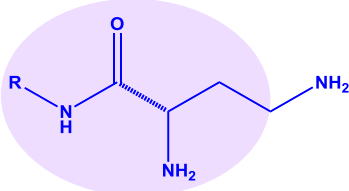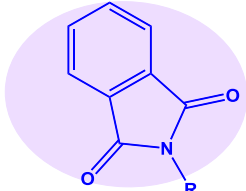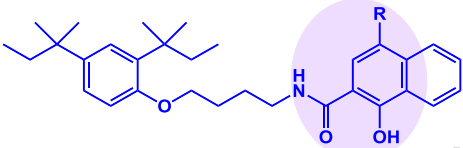
312977		7.48	-4.96725	20
184956		7.47	-1.97039	Not significant
187558		7.45	-4.77675	15
258482		7.45	-4.63639	18
184019		7.44	-6.4521	22
265485		7.4	-4.98476	32

19

ID			
187086	7.39	-7.21694	10
188831	7.39	-8.02652	21
154330	7.38	-5.81937	18
308759	7.38	-4.82741	Not significant
99123	7.37	-5.5936	33
150788	7.37	-6.19569	15
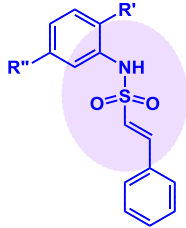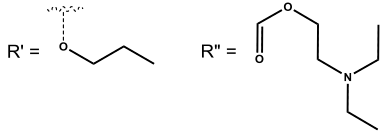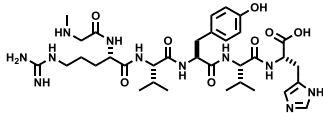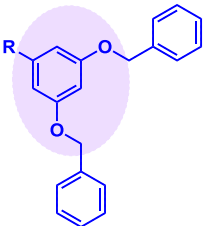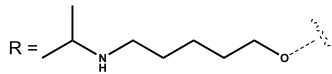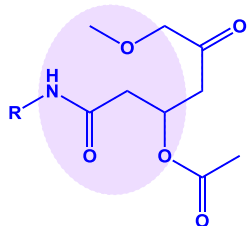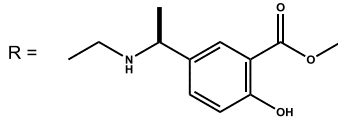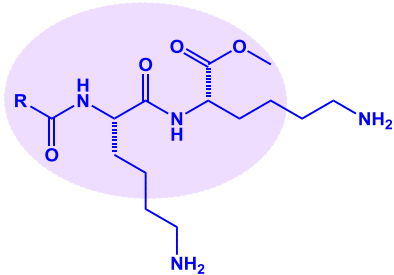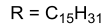
93082		7.36	-4.63786	10
100201		7.36	-2.0712	9
183652		7.36	-6.03565	33
384775		7.36	-5.14933	30
157794		7.35	-3.03283	21
95907		7.34	-5.02586	No quenching

100033		7.34	-4.9311	11
258921		7.34	-4.70569	25
146855		7.32	-4.10071	16

Table S2: Medicinal chemistry data. Chemical names, structures, molecular weight, AlogP, and polar surface area are provided for each class of inhibitor identified in screening against hRRM1.

GRI Number[a]	Chemical Name	Chemical Class (Compound # and abbreviation)	Molecular Weight	AlogP	Polar Surface Area
193480	3,3'-(1,4-phenylenebis (oxy))bis(1-(4-(9H-fluoren-9-yl) piperazin-1-yl) propan-2-ol)	Compound 1 (PB-Piperazine)	722.9136	6.735	71.9
190941	(S)-tetrahydrobenzo [b]thiophen-4-yl)amino-acetamido-diethylmalonate	Compound 2 (tetraHThioDIM)	368.4479	1.435	121.97
95946	(S)-2,4-diamino-N-tetradecylbutanamide	Compound 3 (S-DiTDB)	313.5218	3.671	81.1
183652	N6-(2-(2-(1,3-dioxoisoindolin-2-yl) acetamido)-2-methylpropanoyl)-N2-(4,4,4-trifluoro-3-hydroxy-3-(trifluoromethyl)butanoyl)-L-lysine	Compound 4 (OxoIsoIndoLys)	626.5022	1.161	182.2
384775	(2,4-di-tert-pentylphenoxy)-N-butyl) hydroxy (4-nitrophenoxy) naphthamide	Compound 5 (ButHyNitNap)	612.7551	9.146	113.6

GRI Number[a]	Chemical Name	Chemical Class (Compound # and abbreviation)	Molecular Weight	AlogP	Polar Surface Area
188275	diethylaminoethyl (E) phenylvinyl -sulfonamido- propoxybenzoate	**Compound 6** (DPSP)	460.5863	3.807	93.3
97679	N-methylglycyl- L-arginyl-L-valyl- L-tyrosyl-L- valyl-L-histidine	**Compound 7** (NmetGAVTVH)	743.8535	-3.941	305.6
265485	(3,5-bis(benzyloxy) phenyl-ethyl) amino pentanol	**Compound 8** (BoPEAP)	419.5558	5.438	50.7
166796	methyl 5-((R)-1- ((2-((R)-3-acetoxy- 5-ethoxy-5- oxopentanamido)ethyl) amino)ethyl)- 2-hydroxybenzoate	**Compound 9** (AEOHydBen)	438.4715	0.839	140.3
95889	methyl palmitoyl- Llysyl-L-lysinate	**Compound 10** (MePAMLL)	526.7952	5.548	136.5

a - Univ. of Cincinnati Compound Library reference number

24

Sample preparation for Compounds 1-10 screened in this study:

GRI number[a] (originating source)	Chemical Name	Molecular Weight (parent)	Compound # in this manuscript	Comments for sample preparation
384775 (Salor)	(2,4-di-tert-pentylphenoxy)-N-butyl) hydroxy (4-nitrophenoxy) naphthamide	612.7551	Compound **5**	**BHNaphthamide**
265485 (Panlabs)	(3,5-bis(benzyloxy)phenyl-ethyl)amino pentanol	419.5558	Compound **8**	**BoPEAP**
193840 (Asinex)	3,3'-(1,4-phenylenebis(oxy))bis(1-(4-(9H-fluoren-9-yl)piperazin-1-yl)propan-2-ol)	722.9136	**Compound 1**	Obtained as a powder and was dissolved in DMSO.
169979 (Panlabs)	methyl 5-((R)-1-((2-((R)-3-acetoxy-5-ethoxy-5-oxopentanamido)ethyl)amino)ethyl)-2-hydroxybenzoate	438.4715	Compound **9**	**AEOHydBen**
183652 (Panlabs)	N^6-(2-(2-(1,3-dioxoisoindolin-2-yl)acetamido)-2-methylpropanoyl)-N^2-(4,4,4-trifluoro-3-hydroxy-3-(trifluoromethyl)butanoyl)-L-lysine	626.5022	Compound **4**	**Hexafluoro Lys Phthalimide**
95889 (unknown)	methyl palmitoyl-Llysyl-L-lysinate	526.7952	Compound **10**	**MePAMLL**
188275 (Panlabs)	diethylaminoethyl (E) phenylvinyl-sulfonamido-propoxybenzoate	460.5863	Compound **6**	**DPS Benzoate**
97679 (unknown)	N-methylglycyl-L-arginyl-L-valyl-L-tyrosyl-L-valyl-L-histidine	743.8535	Compound **7**	**NmetGAVTVH**
95946 (unknown)	(S)-2,4-diamino-N-tetradecylbutanamide	313.5218	Compound **3**	*S*-**DiaminoTDBamide**
190941 (Panlabs)	(S)-tetrahydrobenzo[b]thiophen-4-yl)amino-acetamido-diethylmalonate	368.4479	Compound **2**	*tetra***HThioDIM**

Compound 1 (GRI# 193840) was obtained from U. of Cincinnati small molecule library as a white solid and was used after dissolving in DMSO. It was originally obtained from the

Table S3: IC50 measurements of the ten compounds listed in Table 1. See Experimental Methods for the protocol used for deriving IC50 values.

	Specific Activity (nmol min^{-1}mg^{-1})									
Compound	wt R1	5uM	5uM	5uM	Avg (5μM)	100uM	100uM	100 uM	Avg (50μM)	Estimated IC50
1	103.9	63.89	64.2	66.1	64.73	43.07	42.63	40.9	42.2	23.9
2	259.81	177.23	172.93	177.02	175.73	155.94	159.87	162.66	159.49	61.74
3	303.2	261.08	256.33	251.79	256.4	150.87	147.6	149.43	149.3	47.2
4	209.3	155.9	157.3	158.7	157.3	90.1	86.7	86.6	87.8	32.3
5	100.0	85.7	82.9	81.9	83.5	23.4	22.6	22.2	22.74	21.8
6	173	100			100	128.9			128.9	44.0
7	227.31	129.5	126.8	127.46	127.92	103.2	100.9	97.4	100.49	23.6
8	115.78	74.6	69.84	70.93	71.79	47.62	45.55	47.26	46.81	23.6
9	170.58	98.71	100.52	97.8	99.01	80.24	77.86	80.01	79.37	27.2
10	204.3	147.65	151.23	148.42	149.1	94.18	92.71	94.51	93.8	35.7

	wt R1	100uM	100uM	100uM	Avg (100uM)	10mM	10mM	10mM	Avg (10mM)	Estimated IC50
Hydroxyurea	126.46				102.57				67.16	10 76

Table S4: Synopsis of growth inhibition data for all compounds tested in MDA-MB-231 and

HCT-116 cell lines.

Effects	Dose	% Drugs Tested
>50% Growth Inhibition	1μM	0.00%
>50% Growth Inhibition	10μM	8.51%
>50% Growth Inhibition	50μM	36.17%
<50% Growth Inhibition	50μM	63.83%

Table S5: Median effect doses (Dm) for **Compound**, **1**

| | 193840 | Gemcitabine | Gem + 193840 |
	Dm (μM)	Dm (μM)	Dm (μM)
MDA-MB-231	12.241	0.916	0.096
			(2.5 μM 193840)
A549	8.780	0.457	nd
Panc1	7.473	0.615	nd
HCT116	2.045	0.725	0.155
			(1.0 μM 193840)

Table S6: Interactions between **Compound 4** (Phthalimide) and the neighboring atoms in hRRM1. The contacts were found by using a 5 Å cutoff distance. **Compound 4** is designated by chain 1(FFF). The contacts were found by using a 5 Å cut off distance.

1/D/ 1(FFF). / C [C]: /1/A/ 14(MET). / N [N]: 4.91

/1/D/ 1(FFF). / N1 [N]: /1/A/ 49(ALA). / N [N]: 4.66

    /1/A/ 49(ALA). / CA [C]: 4.63

/1/D/ 1(FFF). / O1 [O]: /1/A/ 48(ALA). / CA [C]: 4.27

    /1/A/ 48(ALA). / C [C]: 4.28

    /1/A/ 48(ALA). / CB [C]: 3.30

    /1/A/ 50(GLY). / O [O]: 4.96

    /1/A/ 49(ALA). / N [N]: 3.33

    /1/A/ 49(ALA). / CA [C]: 4.00

    /1/A/ 49(ALA). / C [C]: 4.91

    /1/A/ 50(GLY). / N [N]: 4.65

/1/D/ 1(FFF). / C6 [C]: /1/A/ 49(ALA). / CB [C]:   4.92

/1/A/ 49(ALA). / N [N]:   4.79

/1/A/ 49(ALA). / CA [C]:   4.73

/1/D/ 1(FFF). / O6 [O]: /1/A/ 51(ALA). / O [O]:   4.26

/1/A/ 52(ALA). / CA [C]:   4.86

/1/A/ 52(ALA). / C [C]:   4.30

/1/A/ 53(ALA). / N [N]:   4.23

/1/A/ 52(ALA). / O [O]:   4.47

/1/A/ 53(ALA). / CA [C]:   4.38

/1/A/ 53(ALA). / CB [C]:   4.49

/1/D/ 1(FFF). / O7 [O]: /1/A/ 52(ALA). / C [C]:   4.98

/1/A/ 53(ALA). / N [N]:   4.29

/1/A/ 53(ALA). / CA [C]:   4.15

/1/A/ 53(ALA). / CB [C]:   3.48

/1/D/ 1(FFF). / C9 [C]: /1/A/ 49(ALA). / CB [C]:   4.66

/1/A/ 47(ALA). / O [O]:   4.55

/1/A/ 48(ALA). / CB [C]:   4.66

/1/A/ 49(ALA). / N [N]:   4.56

/1/A/ 49(ALA). / CA [C]:   4.94

/1/D/ 1(FFF). / C10[C]: /1/A/ 49(ALA). / CB [C]:   4.32

/1/A/ 47(ALA). / O [O]:   4.30

/1/A/ 48(ALA). / CA [C]:   4.62

/1/A/ 48(ALA). / C [C]:   4.43

/1/A/ 48(ALA). / CB [C]:   3.59

/1/A/ 49(ALA). / N [N]:   3.61

/1/A/ 49(ALA). / CA [C]:   4.18

/1/D/ 1(FFF). / C11[C]: /1/A/ 49(ALA). / CB [C]:   4.46

/1/A/ 48(ALA). / C [C]:   4.84

/1/A/ 48(ALA). / CB [C]:   4.16

/1/A/ 49(ALA). / N [N]:   3.74

/1/A/ 49(ALA). / CA [C]:   4.05

/1/D/   1(FFF). / C12[C]: /1/A/ 49(ALA). / CB [C]:   4.82

/1/A/ 48(ALA). / C [C]:   4.79

/1/A/ 48(ALA). / CB [C]:   4.06

/1/A/ 49(ALA). / N [N]:   3.64

/1/A/ 49(ALA). / CA [C]:   3.97

/1/D/   1(FFF). / C24[C]: /1/A/ 53(ALA). / N [N]:   4.71

/1/A/ 53(ALA). / CA [C]:   4.66

/1/A/ 53(ALA). / CB [C]:   4.33

Table S7. HRMS for Compounds **1-10**

Compound	Observed Mass	Theoretical Mass
1	722.3819	722.3832
2	ND	368.1406
3	313.3097	313.3093
4	ND	626.1811
5	612.3264	612.3199
6	460.2056	460.2032
7	744.4146	743.4079
8	419.2491	419.2460
9	ND	438.2002
10	526.4492	526.4458

ND = Parent molecular ion not detected.

29

A
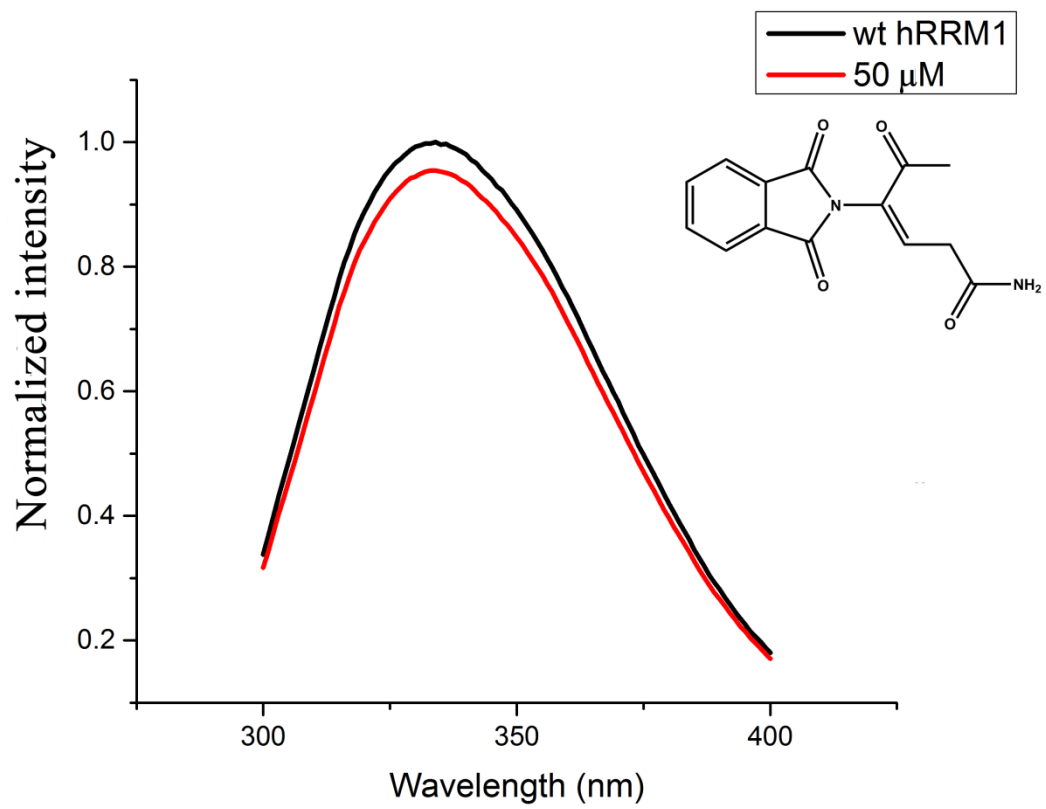
B
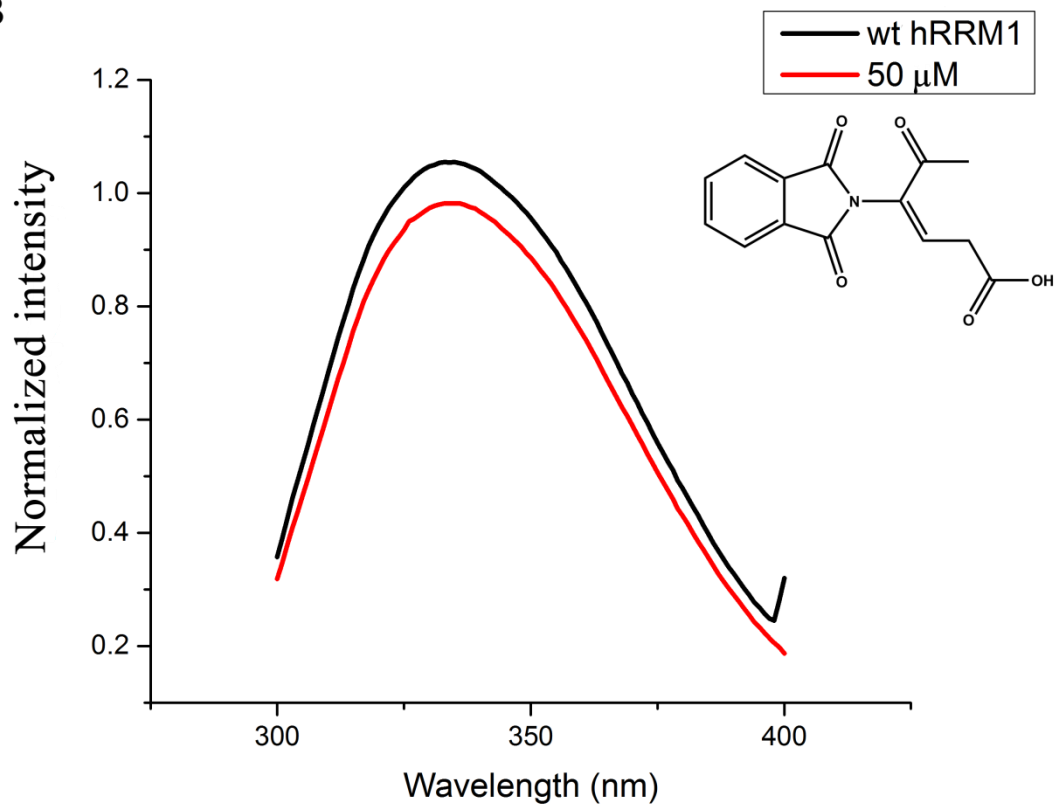
Fig S1. Controls for nonspecific and artificial inhibition in fluorescence quenching assays. Two phthalimide compounds from an unrelated library were chosen for their structural similarity to **Compound 4**. A. (E)-4-(1,3-dioxoisoindolin-2-yl)-5-oxohex-2-enamide shows 5% quenching at 50 µM. B. (E)-4-(1,3-dioxoisoindolin-2-yl)-5-oxohex-2-enoic acid shows 7% quenching at 50 µM.

Fig S2. ^{1}H-NMR data for compounds in Table 1.

Compound 1

Compound 3

29.72   70.28

15 14 13 12 11 10 9 8 7 6 5 4 3 2 1 0 -1 -2 ppm

33

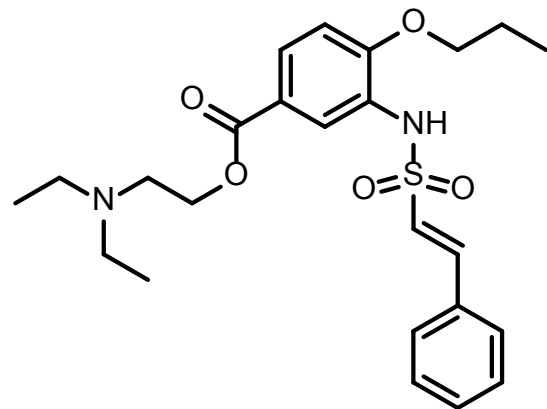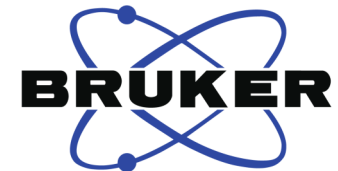Compound 4

Compound 5

Current Data Parameters
NAME   May07-2015-compound7
EXPNO   1
PROCNO   1

F2 - Acquisition Parameters
Date_   20150507
Time   16.51
INSTRUM   spect
PROBHD   5 mm CPPBBO BB
PULPROG   zg30
TD   65536
SOLVENT   Acetone
NS   256
DS   2
SWH   10000.000 Hz
FIDRES   0.152588 Hz
AQ   3.2767999 sec
RG   30.44
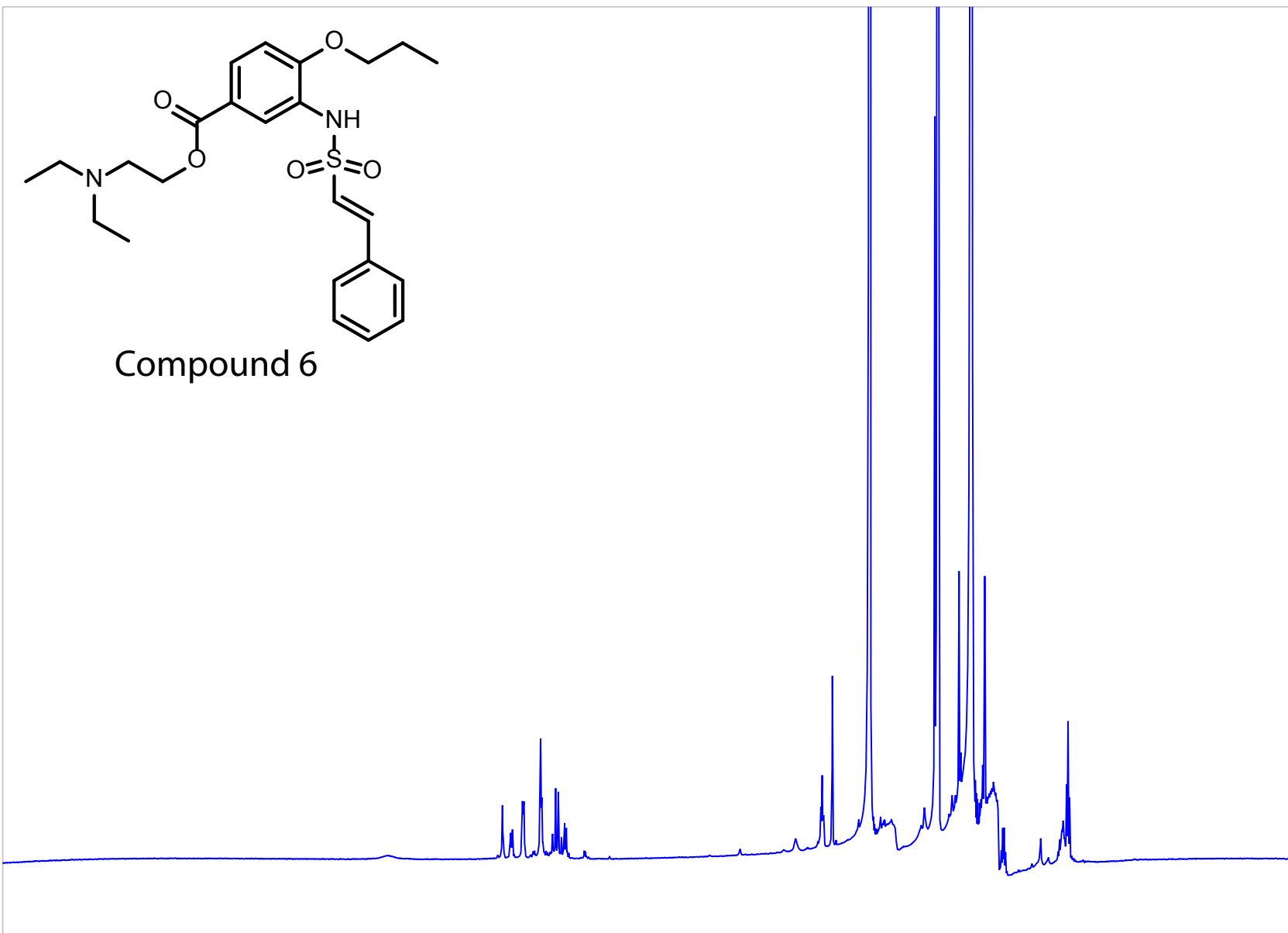DW   50.000 usec
DE   10.00 usec
TE   298.0 K
D1   1.00000000 sec
TD0   1

======== CHANNEL f1 ========
SFO1   500.2430892 MHz
NUC1   1H
P1   11.05 usec
PLW1   15.10000038 W

F2 - Processing parameters
SI   65536
SF   500.2400000 MHz
WDW   EM
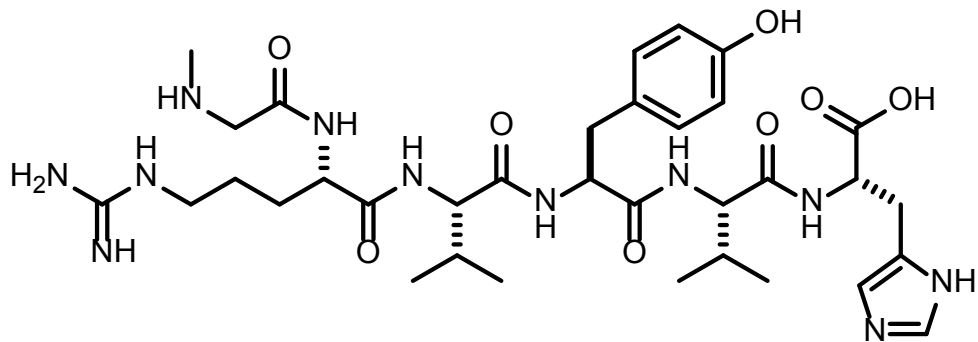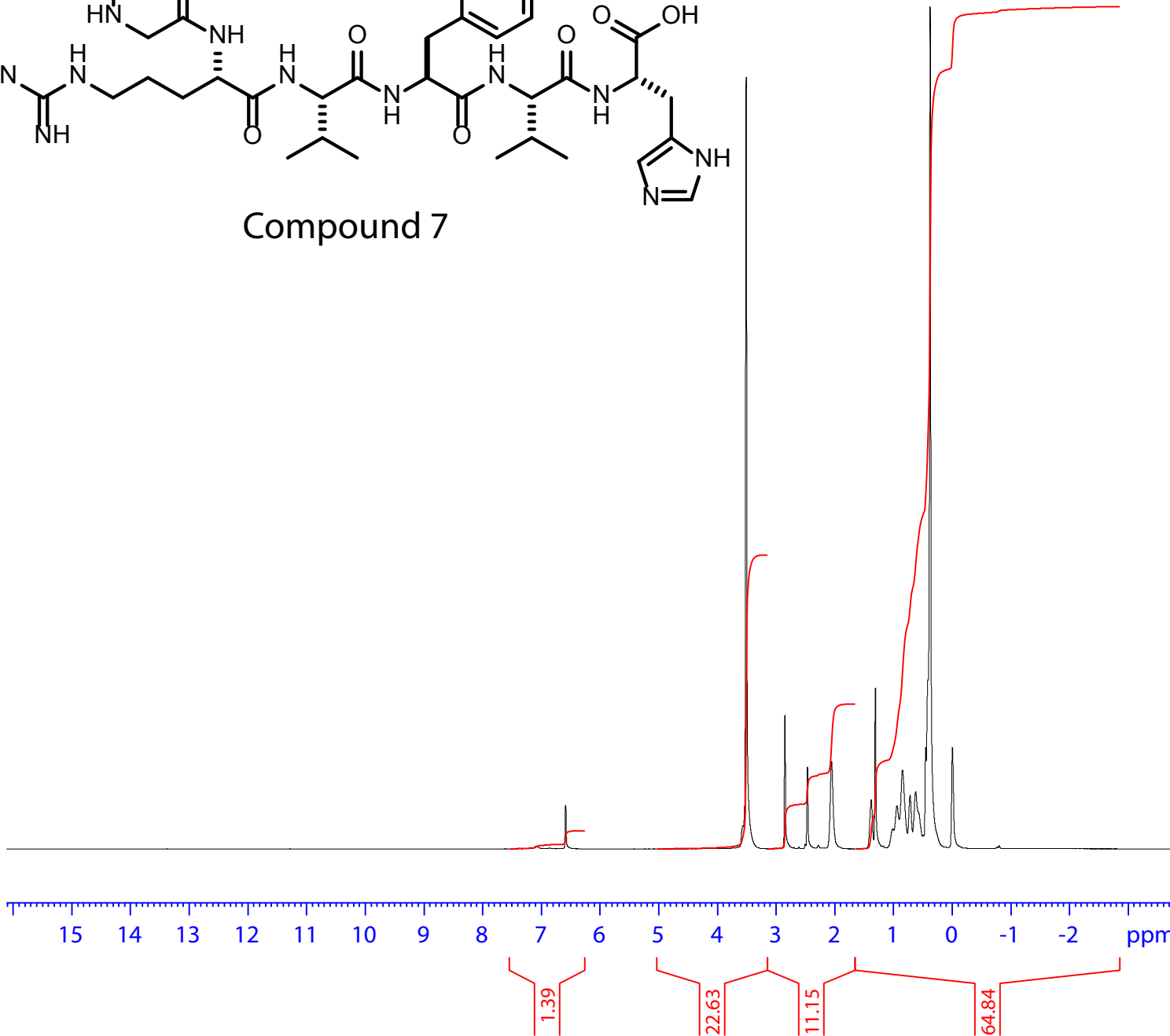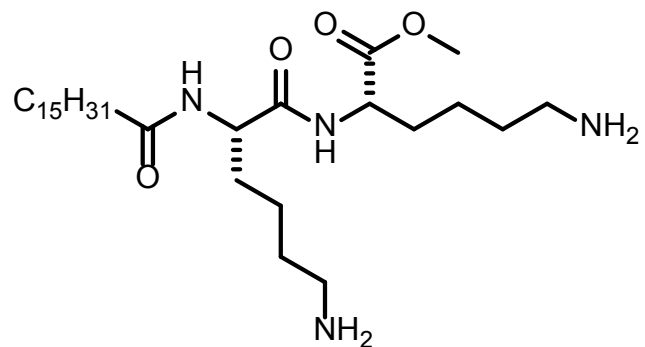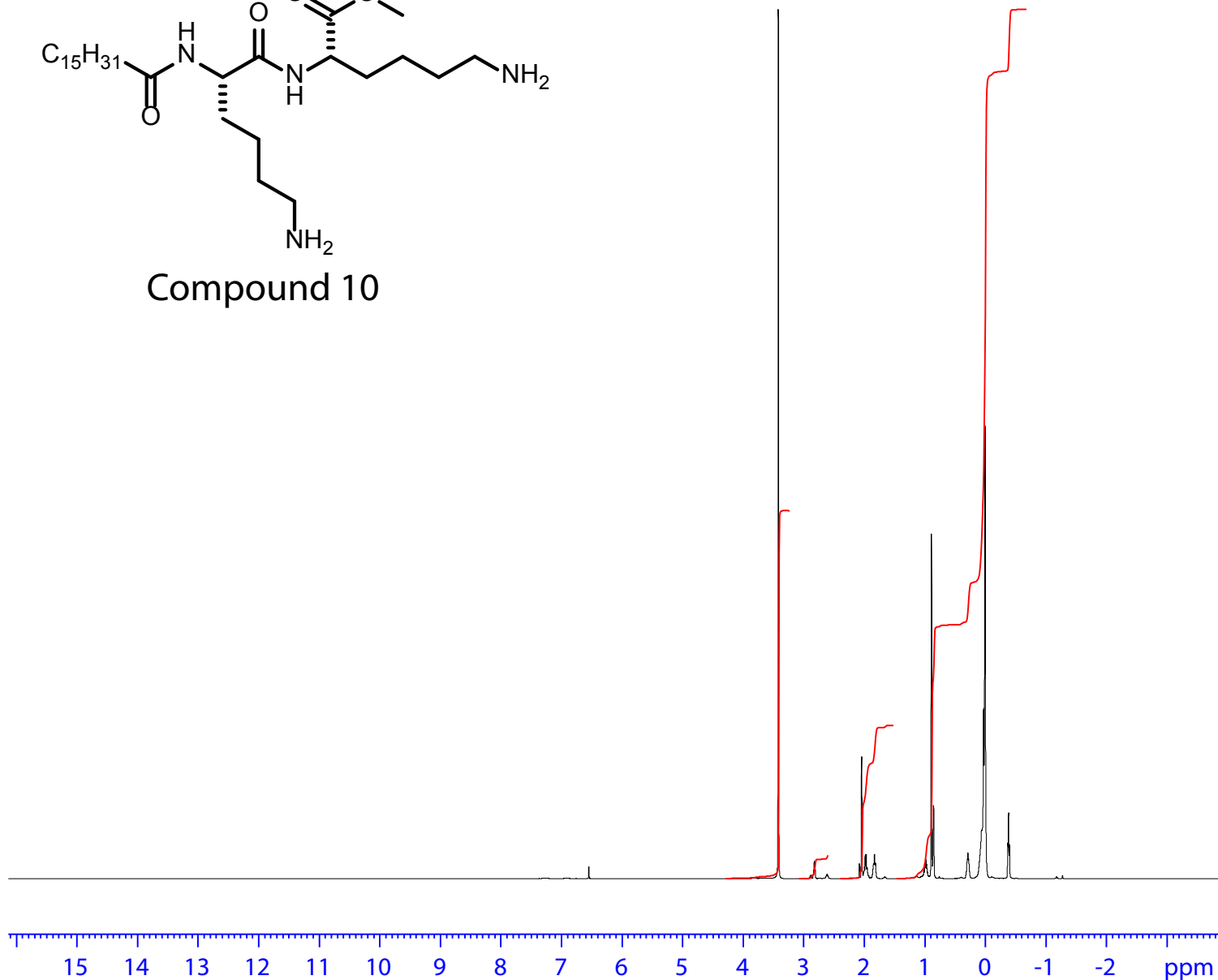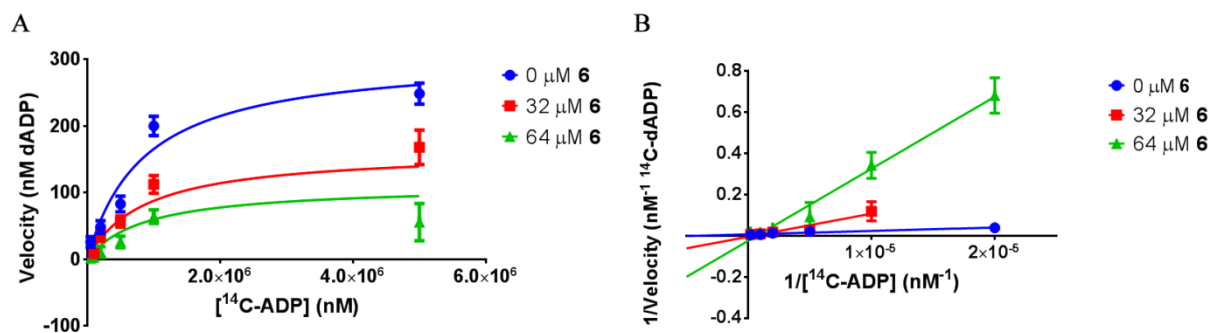SSB   0
LB   0.30 Hz
GB   0
PC   1.00

3.05   3.86   4.97   3.95   14.36   69.80

35

Compound 6

Compound 7

Compound 10

15 14 13 12 11 10 9 8 7 6 5 4 3 2 1 0 -1 -2 ppm

26.01   1.70   10.81   61.48

Fig S3. **Compound 4** is a noncompetitive inhibitor of hRRM1. **A**. A plot of velocity versus [^{14}C-ADP] shows that in the presence of 32 and 64 μM **Compound 4**, velocity does not increase with increasing substrate concentrations after 1 mM, supporting a noncompetitive mechanism. **B**. Double-reciprocal plot for **Compound 4** at 0, 32, and 64 μM. V_{max} changes under all conditions while K_m remains similar for all concentrations of **Compound 4**. An alpha value of 1.047 confirmed that **Compound 4** follows a noncompetitive mechanism.
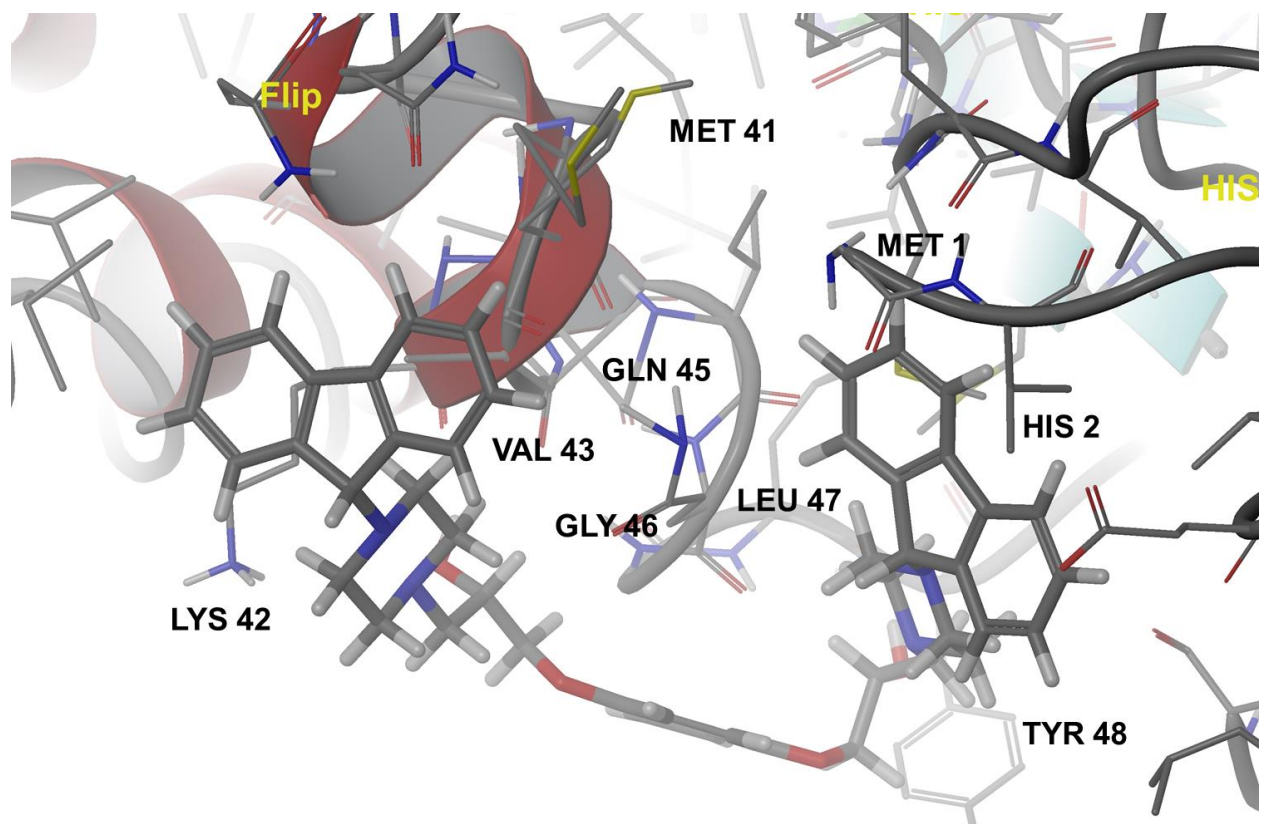
Docking pose Compound **1**
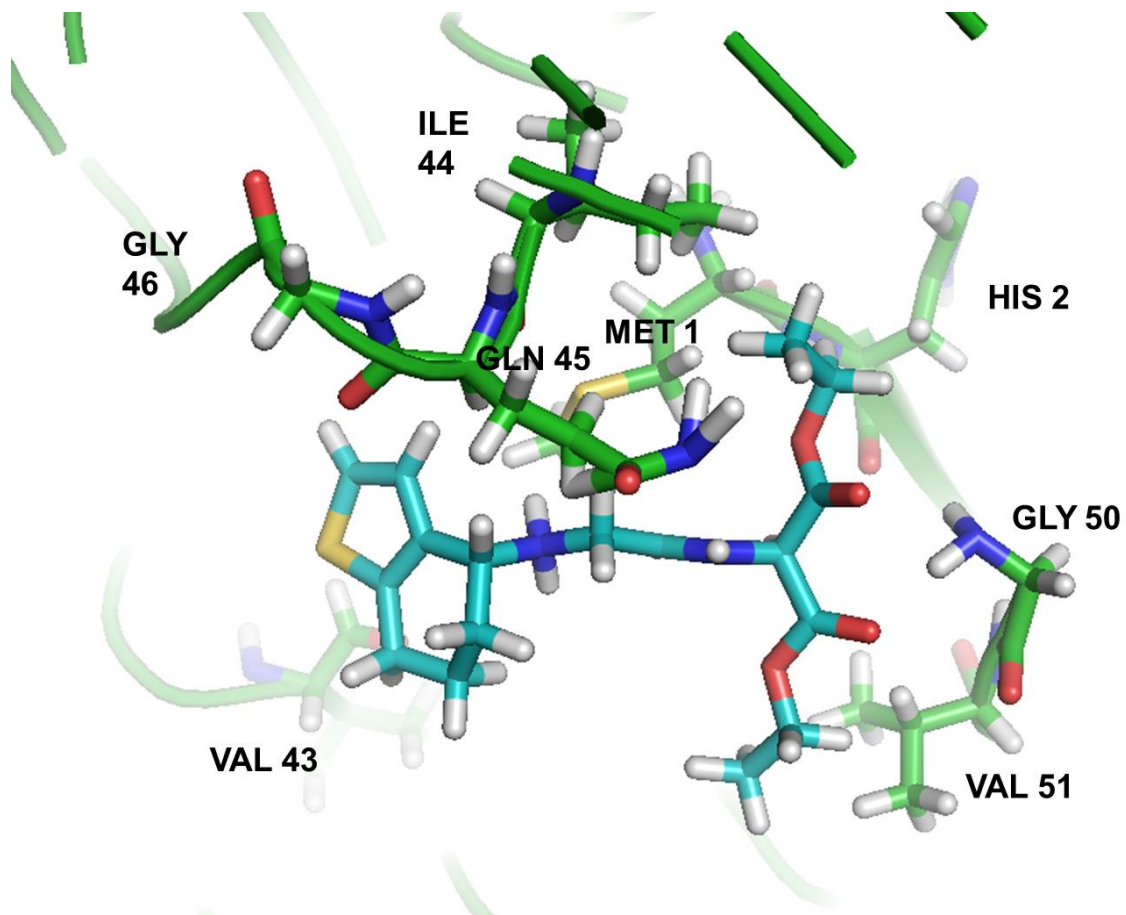
Docking pose Compound **2**
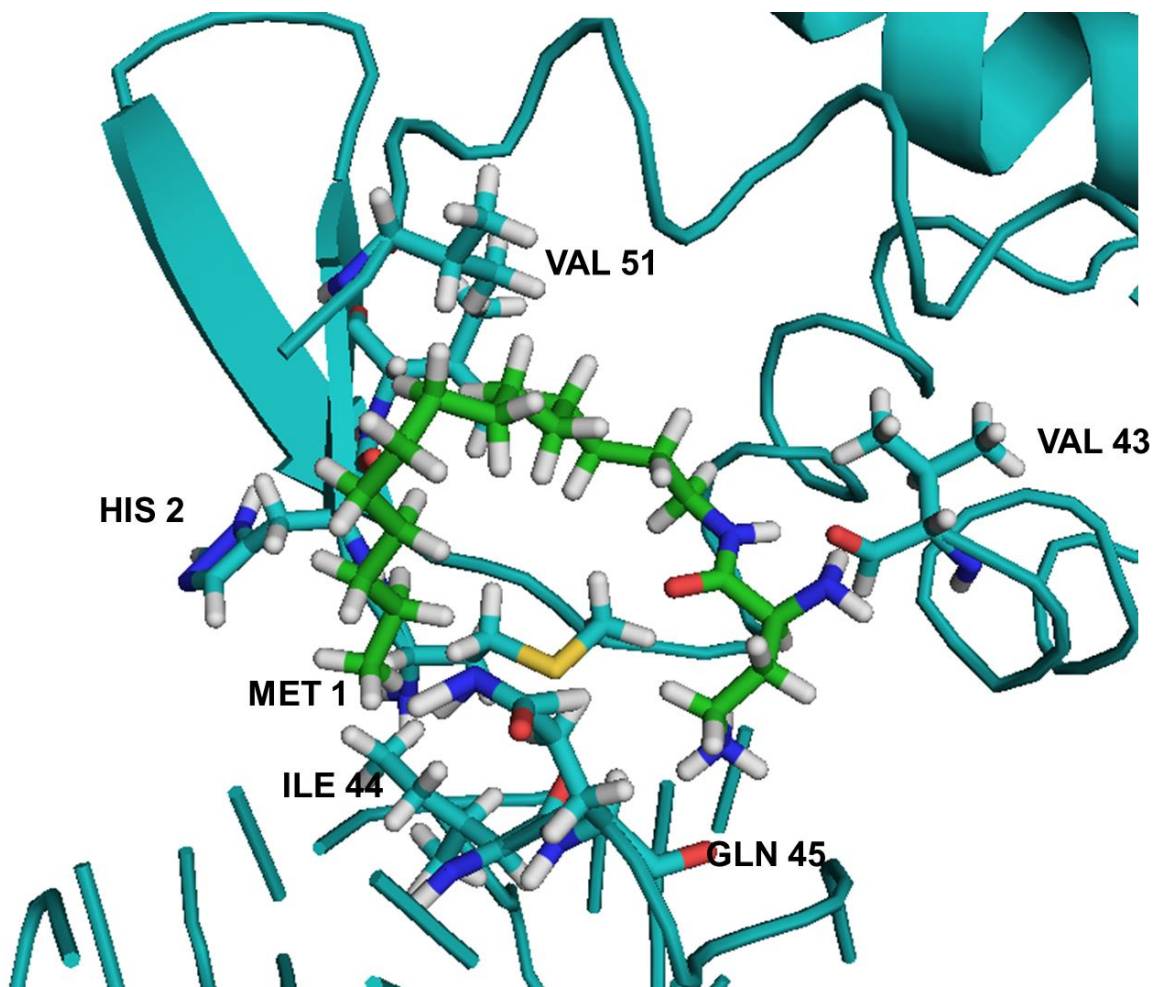
Docking pose Compound **3**
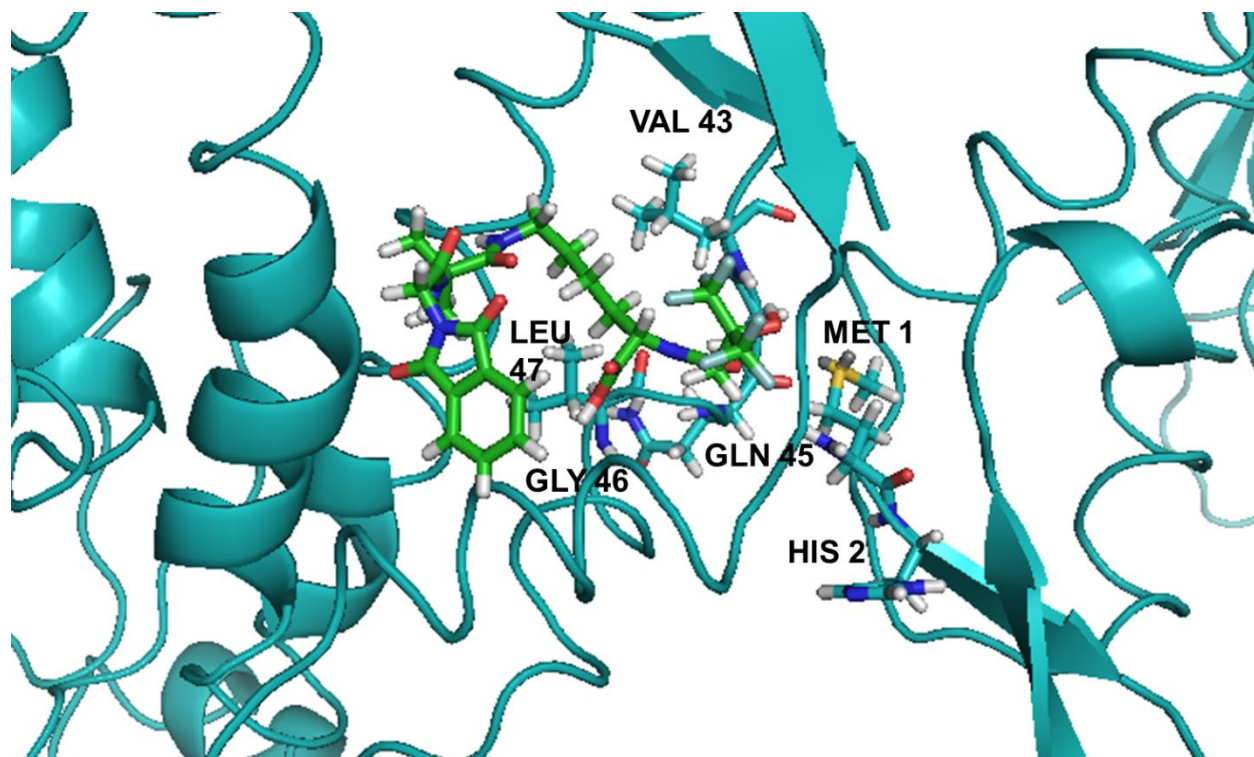
Docking pose for Compound **4**
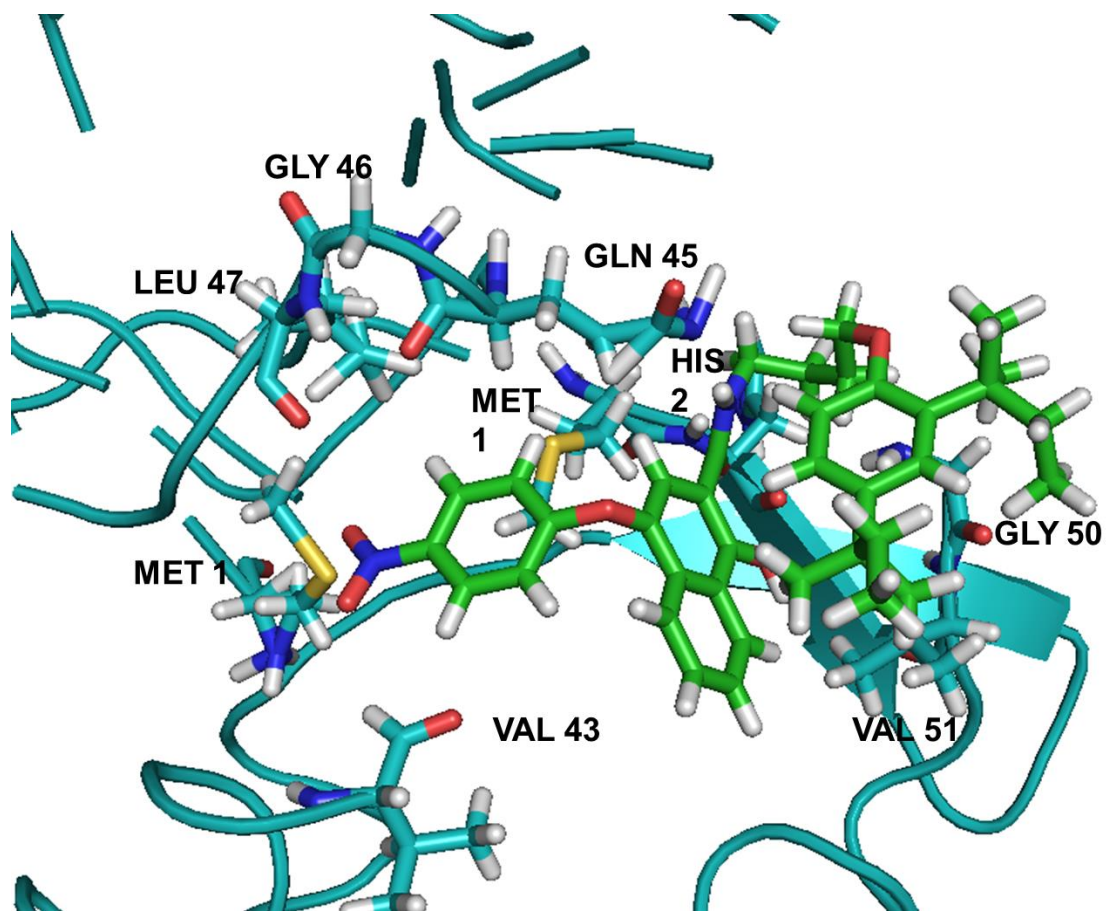
Docking pose for Compound **5**
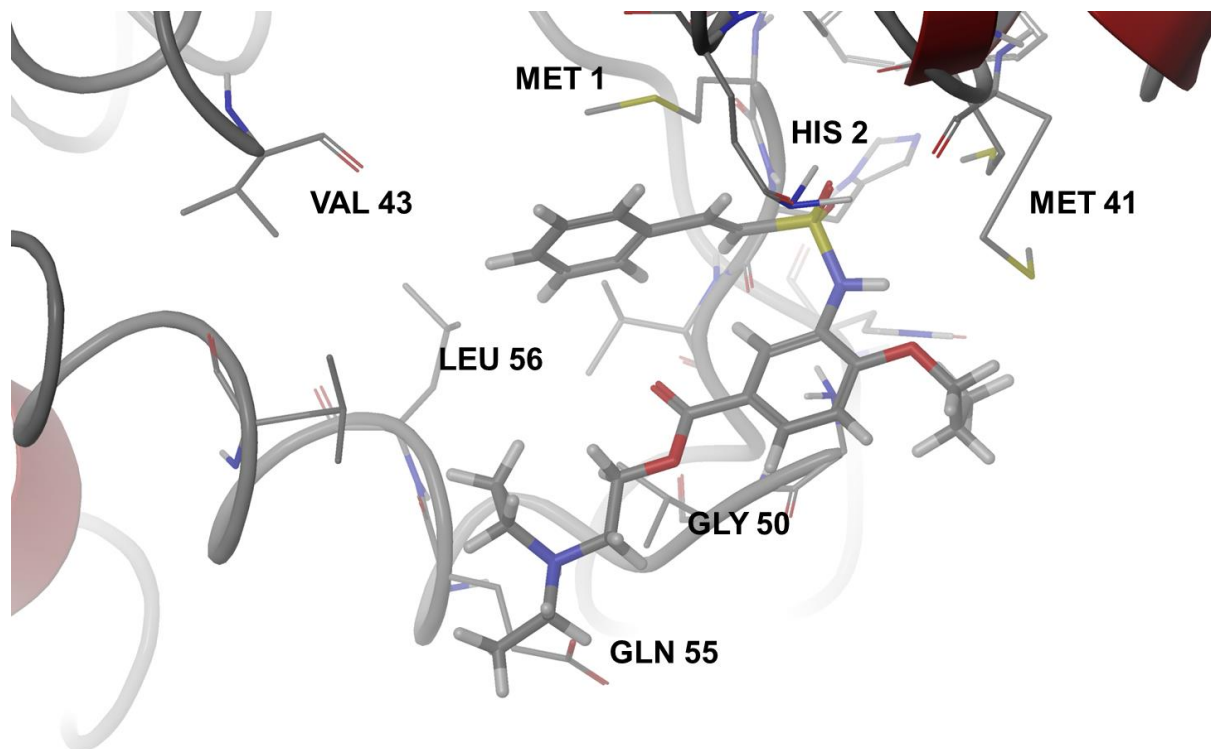
Docking pose for Compound **6**

Docking pose for Compound **7**

Docking pose for Compound **8**
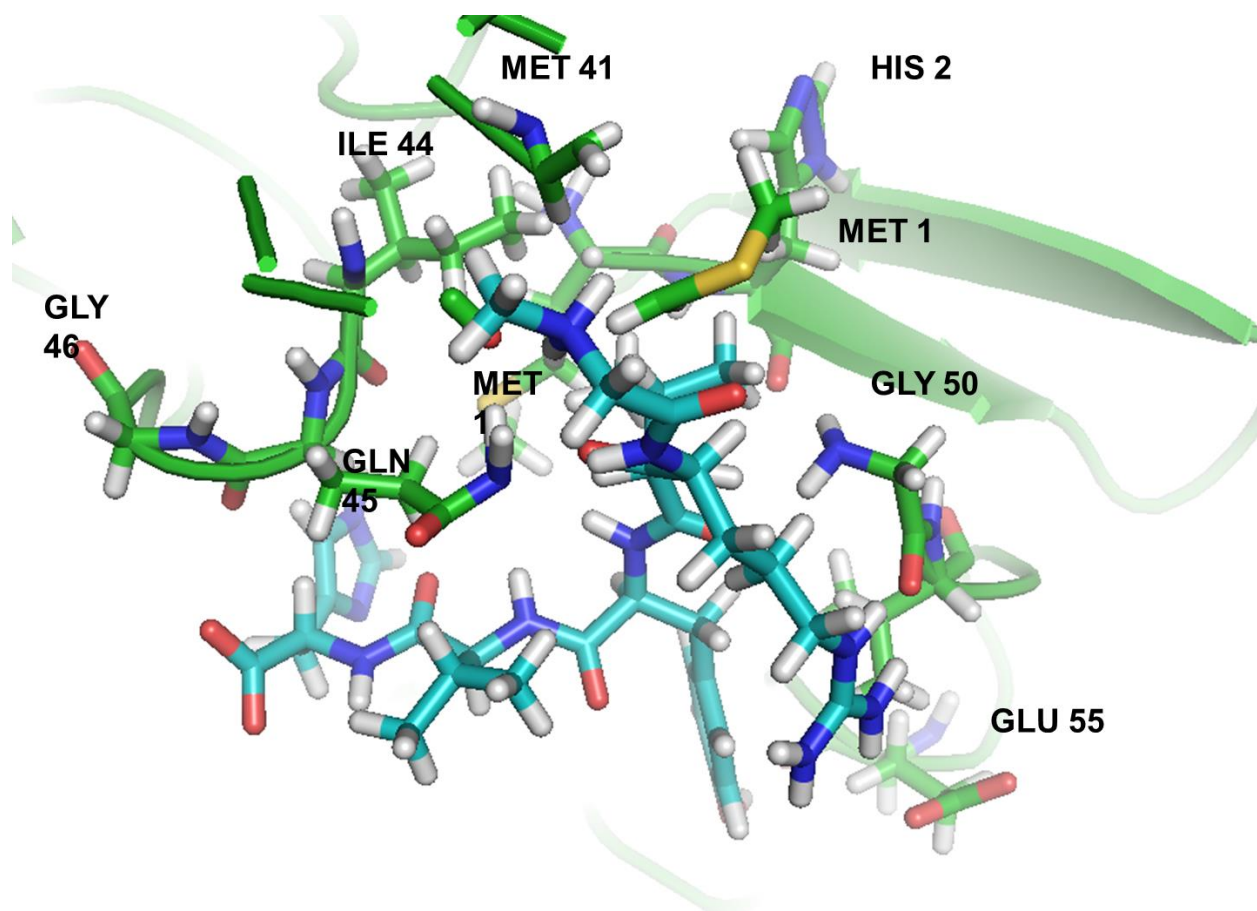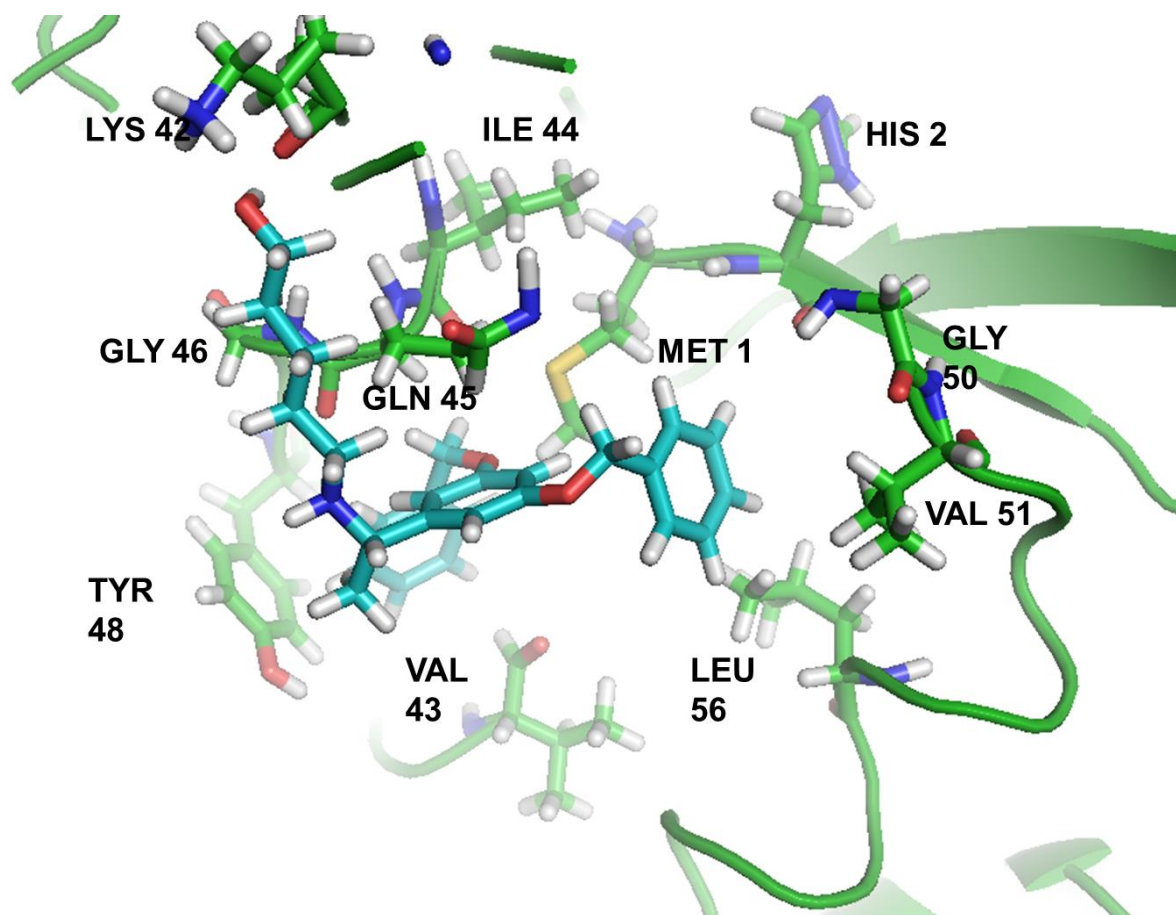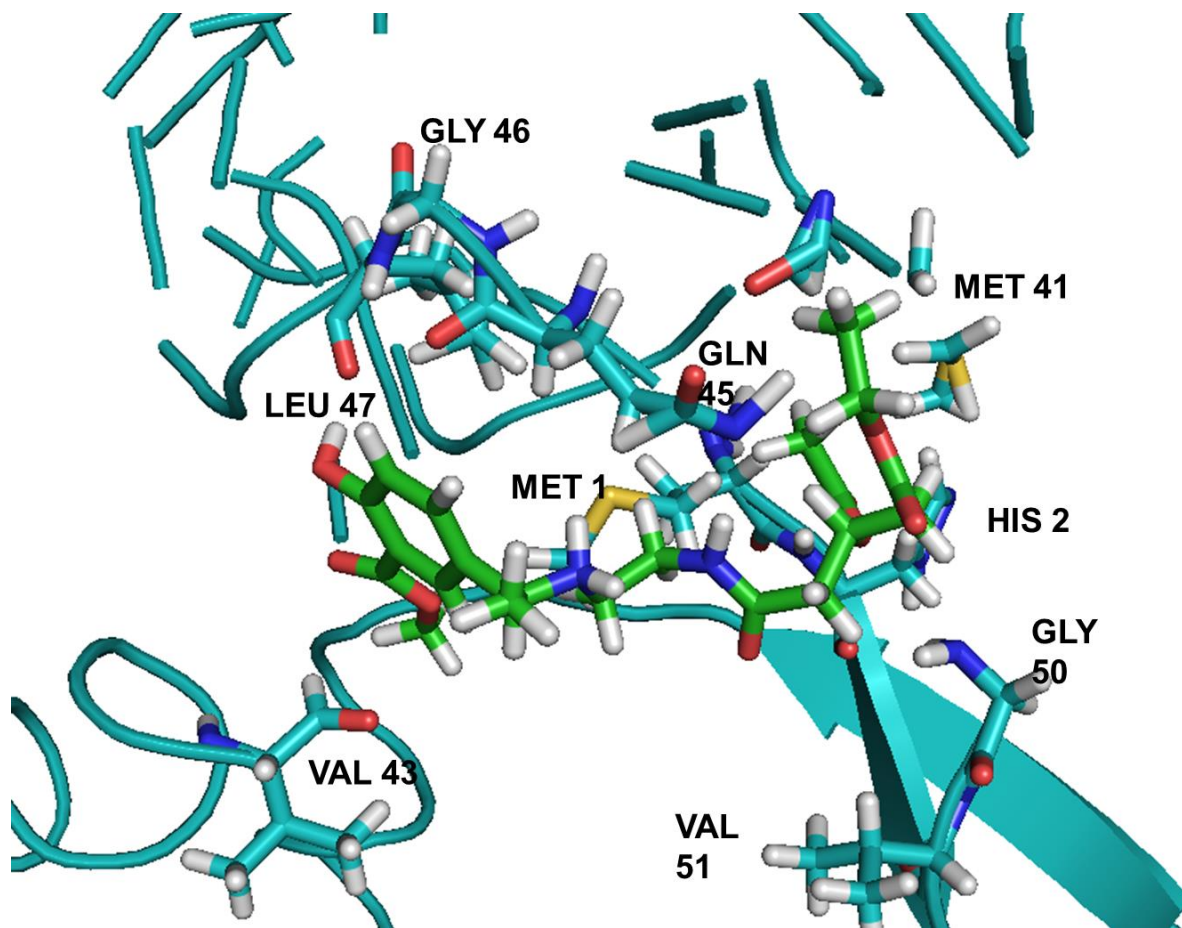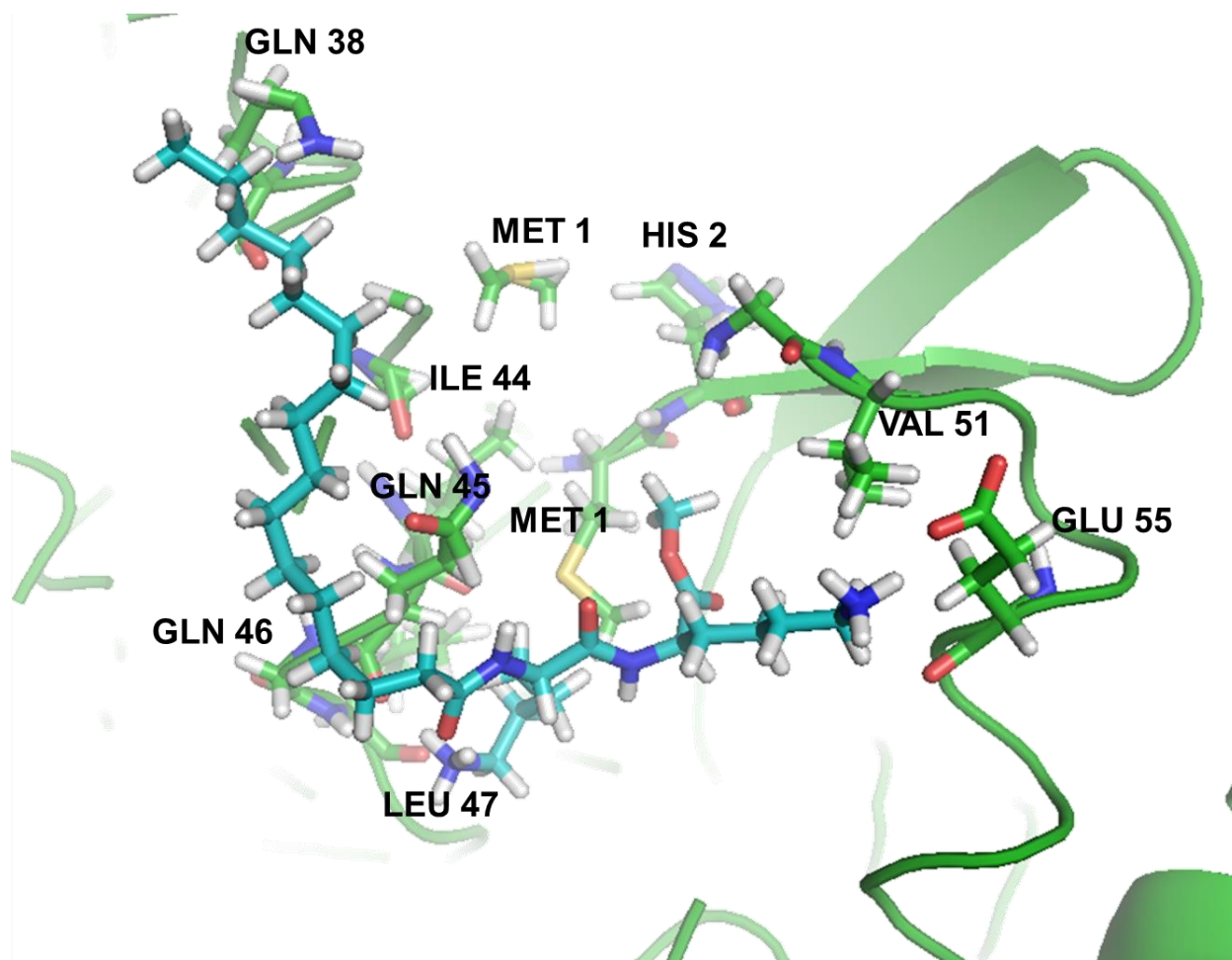
Docking pose Compound **9**

Docking pose Compound **10**

Figure S4. Docking poses of Compounds 1-10. All compounds in Table 1 are shown docked to the M-site. Conserved interactions with Ile 44, Gln 45, Met 1, His 2, Val 51, and Val 43 indicate a consensus binding site.
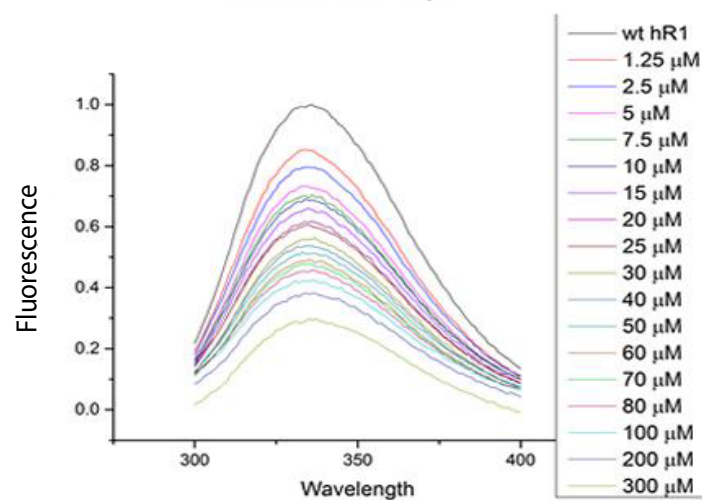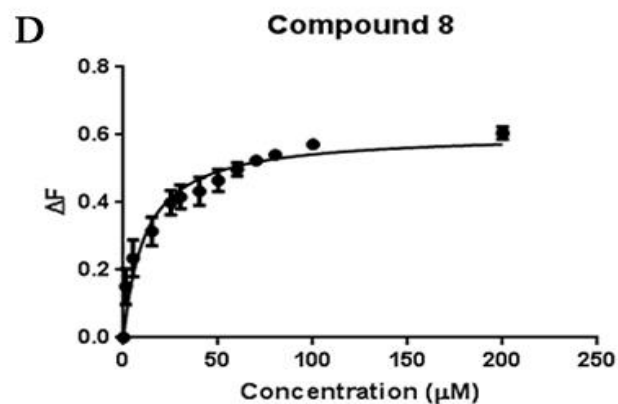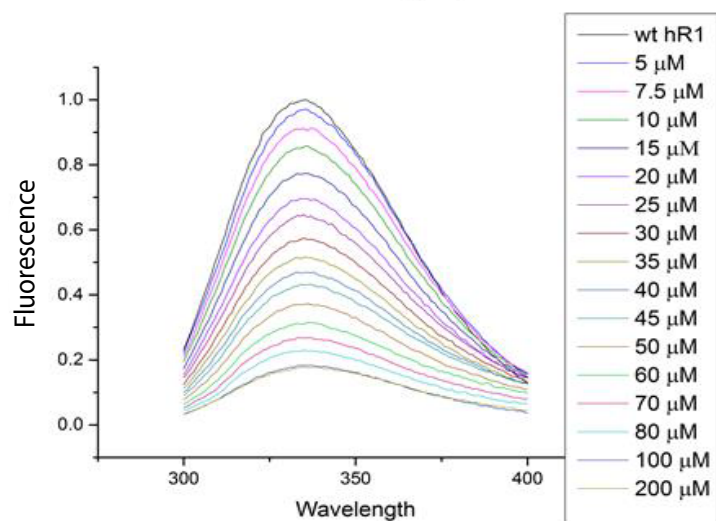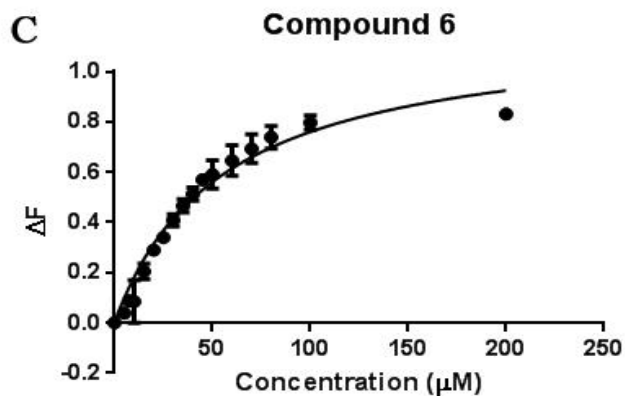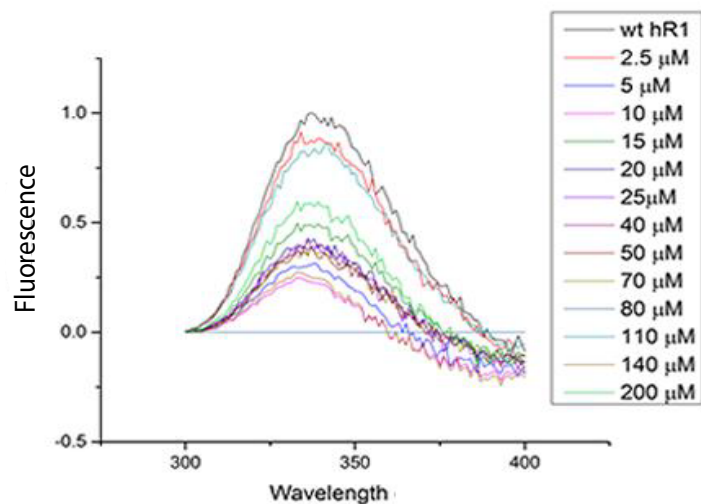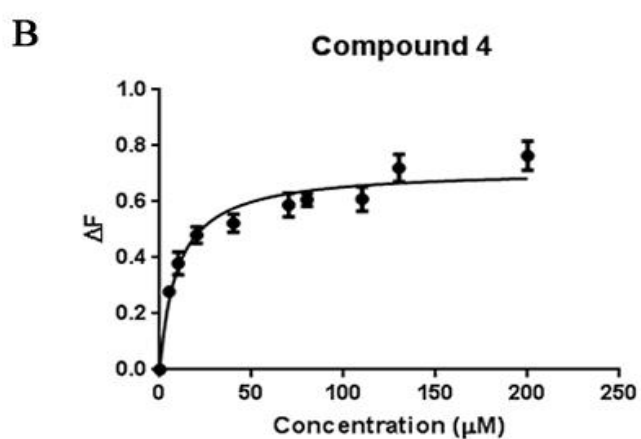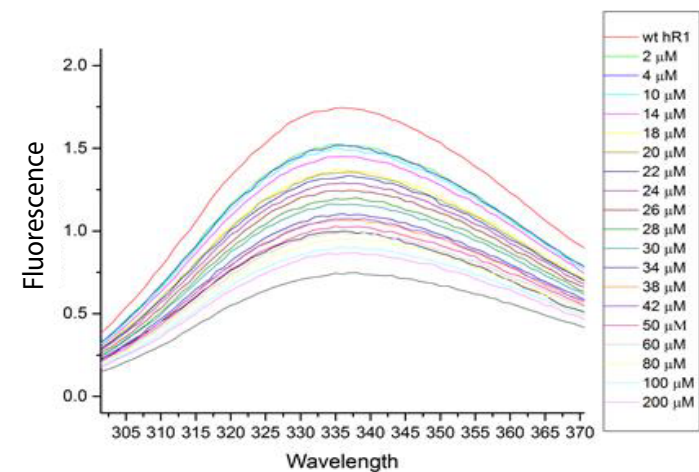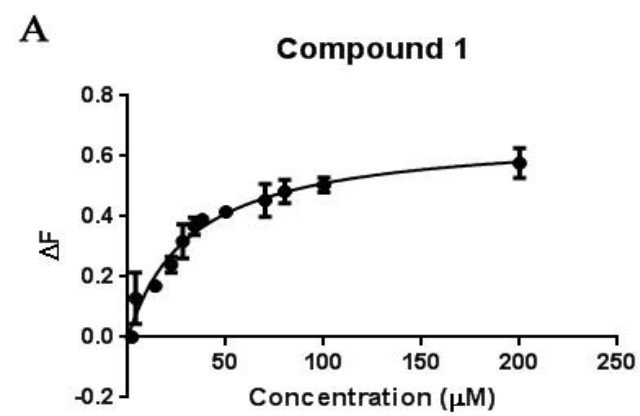
Figure S5. **K$_D$ determination of Compound 1, 4, 6, and 10 by fluorescence quenching.** A. ΔF

plot and absorbance curves for Compound **1,** K$_D$ determineted to be 35.55 ± 3.57. B. ΔF plot and

absorbance curves for Compound **4,** K$_D$ determineted to be 9.69 ± 2.11. C. ΔF plot and

absorbance curves for Compound **6,** K$_D$ determineted to be 55.29 ± 8.25. D. ΔF plot and

absorbance curves for Compound **8,** K$_D$ determineted to be 10.82 ± 1.86.

References

1.   Fairman, J. W.; Wijerathna, S. R.; Ahmad, M. F.; Xu, H.; Nakano, R.; Jha, S.; Prendergast, J.; Welin, R. M.; Flodin, S.; Roos, A.; Nordlund, P.; Li, Z.; Walz, T.; Dealwis, C. G., Structural basis for allosteric regulation of human ribonucleotide reductase by nucleotide-induced oligomerization. *Nat Struct Mol Biol* **2011,** *18* (3), 316-22.

2.   (a) Halgren, T. A.; Murphy, R. B.; Friesner, R. A.; Beard, H. S.; Frye, L. L.; Pollard, W. T.; Banks, J. L., Glide: a new approach for rapid, accurate docking and scoring. 2. Enrichment factors in database screening. *Journal of medicinal chemistry* **2004,** *47* (7), 1750-9; (b) Friesner, R. A.; Banks, J. L.; Murphy, R. B.; Halgren, T. A.; Klicic, J. J.; Mainz, D. T.; Repasky, M. P.; Knoll, E. H.; Shelley, M.; Perry, J. K.; Shaw, D. E.; Francis, P.; Shenkin, P. S., Glide: a new approach for rapid, accurate docking and scoring. 1. Method and assessment of docking accuracy. *Journal of medicinal chemistry* **2004,** *47* (7), 1739-49; (c) Friesner, R. A.; Murphy, R. B.; Repasky, M. P.; Frye, L. L.; Greenwood, J. R.; Halgren, T. A.; Sanschagrin, P. C.; Mainz, D. T., Extra precision glide: docking and scoring incorporating a model of hydrophobic enclosure for protein-ligand complexes. *Journal of medicinal chemistry* **2006,** *49* (21), 6177-96.

3.   Wang, J.; Lohman, G. J.; Stubbe, J., Enhanced subunit interactions with gemcitabine-5'-diphosphate inhibit ribonucleotide reductases. *Proc Natl Acad Sci U S A* **2007,** *104* (36), 14324-9.

4.   Gao, L.; Xu, Y.; Meng, S.; Wu, Y.; Huang, H.; Su, R.; Zhao, L., Identification of the putative specific pathogenic genes of Porphyromonas gingivalis with type II fimbriae. *DNA Cell Biol.* **2012,** *31* (6), 1027-1037.

5.   Shipps, G. W., Jr.; Huang, X.; Deng, Y.; Zhu, L.; Cooper, A. B.; Sun, B.; Achab, A. A.; Lo, S.-M. Preparation of indazole derivatives as ERK inhibitors useful in the treatment of cancer. WO2012087772A1, 2012.

6.   Minor, W.; Tomchick, D.; Otwinowski, Z., Strategies for macromolecular synchrotron crystallography. *Structure Fold Des* **2000,** *8* (5), R105-10.

7.   Emsley, P.; Cowtan, K., Coot: model-building tools for molecular graphics. *Acta Crystallogr D Biol Crystallogr* **2004,** *60* (Pt 12 Pt 1), 2126-32.

8.   (a) Murshudov, G. N.; Vagin, A. A.; Dodson, E. J., Refinement of macromolecular structures by the maximum-likelihood method. *Acta Crystallogr D Biol Crystallogr* **1997,** *53* (Pt 3), 240-55; (b) Adams, P. D.; Afonine, P. V.; Bunkoczi, G.; Chen, V. B.; Davis, I. W.; Echols, N.; Headd, J. J.; Hung, L. W.; Kapral, G. J.; Grosse-Kunstleve, R. W.; McCoy, A. J.; Moriarty, N. W.; Oeffner, R.; Read, R. J.; Richardson, D. C.;

Richardson, J. S.; Terwilliger, T. C.; Zwart, P. H., PHENIX: a comprehensive Python-based system for macromolecular structure solution. *Acta Crystallogr D Biol Crystallogr 66* (Pt 2), 213-21.

9.   Laskowski, R. A., MacArthur,M.W., Moss,D.M., and J.M. Thornton., *PROCHECK*: a program to check the stereochemical quality of protein structures. *Appl. Crystallogr.* **1993,** *26*, 283-290.

10.   Adams, P. D.; Gopal, K.; Grosse-Kunstleve, R. W.; Hung, L. W.; Ioerger, T. R.; McCoy, A. J.; Moriarty, N. W.; Pai, R. K.; Read, R. J.; Romo, T. D.; Sacchettini, J. C.; Sauter, N. K.; Storoni, L. C.; Terwilliger, T. C., Recent developments in the PHENIX software for automated crystallographic structure determination. *J Synchrotron Radiat* **2004,** *11* (Pt 1), 53-5.

11.   DeLano, W. L. *The Pymol Molecular Graphics System*, DeLano Scientific: San Carlos, 2002.

12.   Fairman, J. W.; Wijerathna, S. R.; Ahmad, M. F.; Xu, H.; Nakano, R.; Jha, S.; Prendergast, J.; Welin, R. M.; Flodin, S.; Roos, A.; Nordlund, P.; Li, Z.; Walz, T.; Dealwis, C. G., Structural basis for allosteric regulation of human ribonucleotide reductase by nucleotide-induced oligomerization. *Nature structural & molecular biology* **2011,** *18* (3), 316-22.